Hematopoiesis in numbers

Jason Cosgrove, Lucie Hustin, Rob de Boer, Leïla Perié

Hematopoiesis in numbers

Jason Cosgrove[1*], Lucie Hustin[1*], Rob de Boer[2], Leïla Perié[1]

Author Affiliations

1. Institut Curie, Université PSL, Sorbonne Université, CNRS UMR168, Laboratoire Physico Chimie Curie, Paris, France

2. Theoretical Biology and Bioinformatics, Utrecht University, Utrecht, Netherlands

* both authors contributed equally

Contact information: Leila.Perie@curie.fr

Abstract: Hematopoiesis is a dynamic process in which stem and progenitor cells give rise to the ~10^{13} blood and immune cells distributed throughout the human body. We argue that a quantitative description of hematopoiesis can help to consolidate existing data, identify knowledge gaps, and generate new hypotheses. Here, we review known numbers in murine and, where possible, human hematopoiesis and consolidate murine numbers into a set of reference values. We present estimates of cell numbers, division and differentiation rates, cell size and macromolecular composition for each hematopoietic cell type. We also propose guidelines to improve reporting of measurements and highlight areas where quantitative data are lacking. Overall, we show how quantitative approaches can be used to understand key properties of hematopoiesis.

A quantitative understanding of hematopoiesis

Hematopoiesis is the process by which hematopoietic stem and progenitor cells (HSPCs) give rise to blood and immune cells [1]. Here, we argue that numbers are tools to sharpen our understanding of hematopoiesis [2], but it is challenging and time consuming to find robust values in the literature. Numbers come from various studies and it is rarely discussed how they fit together into our broader understanding of hematopoiesis. To address these issues, we review existing numbers in murine and human hematopoiesis, and generate a set of reference values for murine hematopoiesis. Specifically, we discuss current understanding of cell numbers, division and differentiation rates, cell size and macromolecular composition for each hematopoietic cell type. We also highlight limitations of existing measurements, and instances where quantitative data are lacking. Then using simple calculations, we show how this numerical reference can identify key properties of hematopoiesis and provide suggestions for future research.

How many cells are in the hematopoietic system?

Quantifying absolute cell numbers is important to help contextualize changes that occur in hematopoiesis across lifespan and disease. Here, we summarize current measurements of cell numbers across the major hematopoietic organs, lineages and compartments, focusing on the 16 week old, 22 gram adult female mouse for which we have the most available data (**File S1, Calculation S1a** and [3]). We also summarize known cell numbers in humans. The criteria and sources used to generate reference values are provided in **File S1**, along with metadata for each measurement.

How many cells are there in the hematopoietic organs?

Consolidating cell numbers across the hematopoietic system is non-trivial because (i) cells are heterogeneously distributed across tissues, (ii) differences in sample processing can affect cell yield, (iii) most measurements are expressed in relative rather than absolute terms, and (iv) most numbers come from samples rather than entire tissues. Reviewing existing numbers and accounting for these factors (**Table 1**, **Figure 1, Calculation S1a**), the bone marrow, blood, spleen, lymph nodes and thymus have $4.5x10^8$, $1.6x10^{10}$, $2x10^8$, $7.4x10^7$ and $2.1x10^8$ hematopoietic cells respectively (**Calculation S1a, Table 1**). Adding these values, this gives $1.7x10^{10}$ cells in total – likely an underestimate of the true value, as organs such as the liver and gut are not considered in this calculation.

In humans the standard reference person, historically defined as a male 20–30 years of age, weighing 70 kg and 170 cm in height [4] has ~$1.2x10^{12}$ nucleated bone marrow cells and $2.8x10^{13}$ blood cells (**File S1**) [5]. Surprisingly, direct measurements of human spleen and lymph node cellularity are missing. Assuming the average spleen weighs 130-150g [6] and a single cell weighs 1ng [7], there are ~10^{11} human splenic cells. A 1974 study extrapolating data

from rats to humans reports a total of $1.9x10^{11}$ lymph node lymphocytes [8], distributed amongst 1200 lymph nodes [9]. This reported number of lymph nodes, obtained from a reference digital image library, [9] is much higher than the 460 lymph nodes cited by [8], for which we could find no primary data. The lack of direct measurements of the spleen and the huge range between reported lymph node numbers illustrate that much work is needed to quantify the human hematopoietic system.

How many Hematopoietic Stem Cells are there?

Flow cytometry analyses suggest that murine **HSCs** (Lin^-Kit^+ $Sca\text{-}1^+CD150^+CD48^-$) represent 0.006% of nucleated bone marrow cells and ~16,000 cells in total [10]. However, this is likely to be an overestimate, as a significant proportion (~30-70%) of immunophenotypic HSCs do not meet the functional criteria of **multipotency and self-renewal** [11–13]. In addition, only a subset of HSCs actively contribute to hematopoiesis (**differentiation active**), as determined by **fate mapping** [10,14] and **lineage tracing** [15–17] experiments in mice. **Differentiation active** murine **HSC** numbers range from 2770 to 22,400 [10,18,19]. Given there are 16,000 immunophenotypic **HSCs** in mice and at least 1/3 of Tie2-YFP labelled murine **HSCs** give rise to mature cells, as measured by **fate mapping** [10], we use ~5,200 as a reference value for the number of **differentiation active** murine **HSCs**.

In humans, the number of **differentiation active HSCs** in adults ranges from 25,000-1,300,000 based on inference from **capture-recapture longitudinal genomic analyses of a 59 year-old male** [20] and allele frequency data from a large cohort of blood cancer-free individuals [21]. In a gene therapy context, fewer human **HSCs** (1600-4300) actively contribute to **long-term hematopoiesis post-transplantation**, as inferred from **lentiviral vector integration site** data in patients with **Wiskott-Aldrich Syndrome** [22].

How many hematopoietic progenitors are there?

Downstream of HSCs are the multipotent progenitors (**MPPs**), a functionally heterogeneous population [23], that harbor multi-lineage potential but lack long-term repopulating capacity post-transplantation [24,25]. Flow cytometry measurements report that the **MPP** compartment is ~9 times bigger than the HSC compartment [10], giving $1.4x10^5$ **MPPs** in our reference mouse (**Table 1**).

Downstream of the **MPP** are the **restricted potential progenitors** (**RPPs**) which can be subdivided into the common myeloid progenitors (**CMP),** granulocyte-monocyte progenitors (**GMP)** and megakaryocyte-erythroid progenitors (**MEP**), the common lymphoid progenitors (**CLP**) and the megakaryocyte progenitors (**MkP**). Based on flow cytometry measurements [10,26,27] we compute that for each MPP there are 2.9, 3.6, 5.7,0.2 and 1.8 times more CMPs GMPs, MEPs, MkPs, and CLPs respectively (**Table 1, Calculation S1b)**.

Summing all **HSC, MPP** and **RPP** populations, we estimate that progenitors account for ~0.5% of the murine bone marrow (**Table 1**), while flow cytometry measurements suggest that **lineage negative cells** range from 1-5.7% of total bone marrow [12,28–30]. Taking 4.5% as a representative value [29], we estimate that 4% of bone marrow cells (~18 million cells) are not classically defined progenitors, but don't express mature lineage markers. These cells contain both hematopoietic and non-hematopoietic cells, and remain to be better functionally defined.

In humans, **$CD34^+$ progenitors** (**HSCs**, **MPPs** and **RPPs**) represent an average of 2.5% of all mononucleated bone marrow cells [31,32]. Given the total number of nucleated bone marrow cells from [4], this suggests a total of ~$3x10^{10}$ $CD34^+$ cells in our reference person. Currently, there are conflicting results about the effect of age on the frequency of $CD34^+$ cells [33,34],

and it is unclear to what extent such frequencies change due to gender, ethnicity, and lifestyle factors.

How many mature hematopoietic cells are there?

At the bottom of the hematopoietic hierarchy are the terminally differentiated mature cells. To date, the most extensive measurements in mice account for all mature cells in blood, bone marrow, spleen, thymus, and lymph nodes [35]. For our reference mouse, there are $1.5x10^{10}$ erythrocytes, $1.5x10^{9}$ platelets,$1.6x10^{8}$ myeloid cells, $1.8x10^{8}$ B lymphocytes, and $2.2x10^{8}$ T lymphocytes (**Table 1)**. For megakaryocytes, flow cytometry measurements (0.29% of all nucleated bone marrow cells [36]) suggest a total of $7.7x10^{5}$ cells. Together, this yields a total of $1.7x10^{10}$ mature hematopoietic cells.

In humans, a recent metadata analysis [4] calculates that there are $25x10^{12}$ erythrocytes, $1.5x10^{12}$ platelets, 7×10^{11} T cells, and 3×10^{11} B cells, monocytes $5x10^{9}$ and $6.4x10^{11}$ neutrophils [4], consolidating measurements from human tissue samples along with measurements from rodents and primates where no human data was available.

In tallying hematopoietic cell numbers (**Calculation S1, Table 1**), we find that compartment sizes vary by several orders of magnitude within and between lineages in both mice and humans. Notably, progenitors are much rarer than mature cells (**Figure 2, Table 1**), suggesting that significant cell expansion occurs downstream of the RPP compartment, after lineage commitment has occurred. Quantifying hematopoietic cell numbers is a topic that warrants further experimental focus (see 'outstanding questions'), particularly in humans. When measurements in humans are unavailable, numbers have been extrapolated from rodents. However, cross-species measurements highlight important differences calling for carefulness,

for example myeloid cells account for ~9-16% of all blood leukocytes in our reference mouse [3,35], but in humans this number is ~65% [6]. Total cell numbers can help to understand how hematopoiesis changes during disease, complementing other resources such as the human cell atlas, and facilitating cross-species comparisons to understand how the hematopoietic system has evolved.

How many hematopoietic cells do we produce per day?

The rates at which cells divide, differentiate and die are key regulators of cell numbers [10,14], and if perturbed can lead to hematological malignancies [37]. In the following section we discuss current understanding of these parameters, excluding T-cells that have been reviewed elsewhere [38].

Division rate and division number

Division rates can be measured using **division-linked dilution assays**, or reporter molecules that incorporate into newly synthesized DNA [39]. In mice, HSCs are reported to divide every 145 days [40]. These values are on the same order of magnitude as estimates derived from **fate-mapping** studies [10,14]. However the reported proportion of cells entering S-phase per unit time, using a BrdU EdU sequential labelling technique, suggests a proliferation rate of approximately once every 4 days [41]. Presumably these differences in reported values arise due to differences in labeling techniques or heterogeneity within **HSCs** [14,41,42]. In mice, MPPs reportedly cycle faster than HSCs [14,43] *in vivo* EdU labeling showed that cycling rates for RPPs are higher than those measured in MPPs [43]. These data are consistent with a linear amplification model where proliferation rates increase with early maturation[14]. In humans, HSCs have been estimated to divide once every ~280 days, a value inferred by mathematical modelling of X chromosome inactivation patterns in females [44]. Division rates for human MPPs, and RPPs *in vivo* are lacking however.

Despite recent progress in our ability to quantify division rates, the number of divisions it takes to differentiate an HSC into a mature cell is unknown. Knowing the size of each cell compartment, it is possible to estimate the minimum number of divisions in this process (Figure 3 **Calculation S2a**). Performing this estimation in mice suggests that at least 15-22 divisions are needed to account for the expansion of 5200 HSCs to 10^8-10^{10} mature cells (Figure 3 **Calculation S2a**), with erythropoiesis requiring ~7 more divisions than myelopoiesis. Considering the fraction of B cells that survive after negative and positive selection, we estimate a minimum of 20 divisions are needed to produce all mature B cells (**Figure 3 Calculation S2b**). We estimate that megakaryocytes derive from HSC in 7 divisions (**Figure 3 Calculation S2c**), not including **endomitoses** and produce on average 519 platelets each day (**Calculation S2d**). Importantly, these estimates don't consider HSC heterogeneity in clonal expansion, nor the impact of cell death and differentiation, processes that are discussed below.

Lifespans and turnover rates

A key parameter which regulates cell numbers is the rate of cell death, which can be derived from half-life and lifespan measurements (**Table 2**). Half-life measures are mathematically inferred by following the loss of a label over time within a cell population. Cells can be labelled *in vivo* with BrdU, EdU, deuterium isotope or *ex vivo* [45]. Half-lives have not been measured *in vivo* in progenitor populations, as no labelling methods can currently discriminate between death and differentiation. In mature cell types of both humans and mice, results show that most cells are short-lived - on the order of days or weeks (**Tables 2-3**), with some variation within cell types due to maturation or activation state [45] and tissue localization [46].

While measuring death rates is challenging, estimation of turn-over can help to understand the dynamics of hematopoiesis (Calculation S2e). In steady state conditions, the turnover rate of

each lineage can be estimated from population sizes and circulating half-lives (**Tables 2-3**), assuming that cell production and death rates balance each other (Figure 3, **Calculation S2e**). In mice, despite different population sizes, erythroid and granulocyte turnover rates are on the same order of magnitude due to large differences in lifespan (35 days [47] versus 1.2 days [46], **Calculation S2e**). Murine B-lymphocytes however have a 10-fold lower turnover rate (**Calculation S2e**), consistent with the relatively low number of CLPs. Importantly, the steady state assumption we make is not always valid; different studies report that the number of phenotypic HSCs in mice increases with age [48,49].

In humans, it has been estimated that $3.3x10^{11}$ cells are produced each day, ~85% of which are hematopoietic [4]. $2.1x10^{11}$ of these cells are erythroid, $6x10^{10}$ are neutrophils, $1.5x10^{9}$ are monocytes and $7x10^{9}$ are lymphoid (**Table 3**) [4]. In this study, platelets were not considered a cell type and so were not included in the final analysis. Based on available measurements of total platelet numbers ($1.5x10^{12}$) as well as lifespan (9.9 days) [50], we estimate a turnover rate of $1.5x10^{11}$ platelets per day (**Table 3**). In humans, as in mice, the erythromyeloid lineages dominate cell turnover.

Differentiation rates

Apart from division and death rates, the residency times *within*, and transition rates *between* compartments regulate cell dynamics. Inference from a murine **fate mapping** study reports that differentiation rates increase from HSC to MPP and RPP [10], and that an individual MPP is 180 times more likely to transition into a CMP than a CLP. While the confidence intervals around these estimates are large, they suggest that lymphoid commitment is rare. Based on these values of MPP to CLP transition[10], a scRNAseq dataset of 1000 murine MPPs contains only 5-6 cells that commit to the lymphoid fate, highlighting the need for enrichment strategies to study early lymphopoiesis [51]. However, it is important to note that estimates derived from

fate mapping studies vary depending on technical factors such as the labelling system, the gating strategy, or the model used in parameter fitting [14]. In humans, there are no reported *in vivo* differentiation rates, although retrospective **lineage-tracing** methods that make use of endogenous barcodes within the genome (e.g. somatic mutations) are emerging [20].

To summarize, hematopoietic cells are short-lived, and must be constantly regenerated. In both mice and humans, the number of myeloid and erythroid cells produced each day are of the same order of magnitude, even though there are far more erythroid than myeloid cells when we consider total cell numbers. This is due to large differences in their expected lifespan.

How big are different hematopoietic cell types? What does each cell type comprise?

As hematopoietic cells differentiate, they undergo significant remodeling, changing their shapes, sizes and macromolecular composition to fulfill specialized functions, such as oxygen transport, blood clotting, and pathogen killing.

Cell size can be measured using synthetic beads as an internal control in flow cytometry, or by imaging [52] and results show that cell volumes vary dramatically between cell types (**Table S1**). For example, murine HSCs, CMPs, GMPs and MEPs have a volume of 175 μm^3, 210 μm^3, 320 μm^3 and 450 μm^3, respectively [53]. Differences in cell size impact cellular composition with protein and lipid numbers scaling linearly with cell volume for many mature blood cell types **(Table S1, Figure S2).** As a consequence, quantitative differences in cell size can have major implications for biosynthesis when we consider the large numbers of cells produced each day (see above). Aside from the quantification of protein synthesis rates in progenitors [54], measurements of the ATP and macromolecular requirements for hematopoietic cell production are lacking. However, newly-developed high-sensitivity mass spectrometry-based approaches

241 are emerging to tackle this issue [55]. Using the relative protein content of the different cell
242 types (**Table S1**) and the number of cells produced in humans per day (**Table 3**), we compute
243 the amount of protein and ATP required to fuel cell turnover (**Calculation S2f**). This
244 calculation predicts that myelopoiesis requires ~2.8 times more ATP than erythropoiesis in
245 humans, considering only protein synthesis requirements.
246
247 To summarize, each hematopoietic cell type has a distinct size and shape, helping them to fulfill
248 specialized functions. Consequently, the amount of energy and biomaterial it takes to
249 regenerate each cell type may vary significantly, but many parameters have yet to be quantified.
250 Quantitative hematometabolism is a research topic that warrants further focus, and may
251 facilitate the development of novel dietary interventions to modulate hematopoiesis.
252

253 **Concluding remarks**

254 In this article we have summarized key numbers in hematopoiesis, providing a quantitative
255 reference for the field, and highlighting areas where quantitative information is missing. These
256 numbers can be accessed and updated at the Bionumbers repository
257 *(https://bionumbers.hms.harvard.edu/)*.
258
259 In reviewing existing numbers, we learn that in mice, 5.2 x 10^3 HSCs give rise to 10^{10}
260 hematopoietic cells while in humans 10^4-10^6 HSCs give rise to 10^{13} mature hematopoietic cells.
261 Strikingly, in both humans and mice most hematopoietic cells are short-lived – on the order of
262 days or weeks – as such hematopoiesis accounts for 90% of total blood cell turnover [4]. We
263 have also reviewed what is known about hematopoietic cell size and composition, with
264 numbers revealing that each cell type is likely to have very distinct metabolic requirements.

For example, we estimate that at least ~36kcal per day, the equivalent of a single strawberry, is needed to maintain RBC homeostasis in humans (Figure S3, **Calculation S2g**). This value is surprising low, given RBCs account for 90% of all cells in the human body, and arises due to the relatively low protein content and low ATP turnover rate of RBCs compared to other cell types.

We also illustrate how quantitative approaches may improve our ability to: (i) design experiments, as illustrated earlier by the need for novel enrichment strategies to study early lymphopoiesis (ii) consolidate and contextualize data across studies and species, identifying knowledge gaps (see 'outstanding questions') and to (iii) make novel predictions about how hematopoiesis is regulated.

In generating reference values, it is important to understand how each measurement has been made. Conflicting values in the literature may arise due to nuanced technical details about sample processing and analysis, and may irreflective of true biological variation. Unfortunately, many numbers could not be included in this article due to poor reporting with unclear tissue processing and data transformation. We suggest that best practice is to make raw data available for each figure, along with associated metadata about sample processing, data acquisition and analysis steps.

To summarize, hematopoiesis is a dynamic process, giving rise to diverse cell types with distinct population sizes, tissue localization, turnover rates, and sizes. We hope that this article illustrates how quantitative approaches can improve our understanding of hematopoiesis, and anticipate that the numbers presented can serve as a reference starting point for the immunology and hematology scientific communities.

Acknowledgements:

We thank all the Perié lab members, Rob Phillips, Lucie Laplane and Rob Signer for giving their feedback on the manuscript. This work was supported by grants from the *Labex Cell(n)Scale* (ANR-11-LABX-0038, ANR-10-IDEX-0001-02 PSL) (to L.P.). This work is part of a project that has received funding from the European Research Council (ERC) under the European Union's Horizon 2020 research and innovation programme 758170-Microbar (to L.P.) J.C. was supported by a Foundation ARC fellowship.

References

1 Sender, R. *et al.* (2016) Revised Estimates for the Number of Human and Bacteria Cells in the Body. *PLOS Biol.* 14, e1002533

2 Milo, R. and Phillips, R. (2015) *Cell Biology by the Numbers*, 1 edition.Garland Science.

3 Grubb, S.C. *et al.* (2009) Mouse Phenome Database. *Nucleic Acids Res.* 37, D720–D730

4 Sender, R. and Milo, R. (2021) The distribution of cellular turnover in the human body. *Nat. Med.* 27, 45–48

5 Lahoz-Beneytez, J. *et al.* (2016) Human neutrophil kinetics: modeling of stable isotope labeling data supports short blood neutrophil half-lives. *Blood* 127, 3431–3438

6 Valentin, J. (2002) Basic anatomical and physiological data for use in radiological protection: reference values: ICRP Publication 89. *Ann. ICRP* 32, 1–277

7 Makarieva, A.M. *et al.* (2008) Mean mass-specific metabolic rates are strikingly similar across life's major domains: Evidence for life's metabolic optimum. *Proc. Natl. Acad. Sci. U. S. A.* 105, 16994–16999

8 Trepel, F. (1974) Number and distribution of lymphocytes in man. A critical analysis. *Klin. Wochenschr.* 52, 511–515

9 Qatarneh, S.M. *et al.* (2006) Three-dimensional atlas of lymph node topography based on the visible human data set. *Anat. Rec. B. New Anat.* 289, 98–111

10 Busch, K. *et al.* (2015) Fundamental properties of unperturbed haematopoiesis from stem cells in vivo. *Nature* 518, 542–546

11 Wilson, N.K. *et al.* (2015) Combined Single-Cell Functional and Gene Expression Analysis Resolves Heterogeneity within Stem Cell Populations. *Cell Stem Cell* 16, 712–724

12 Challen, G.A. *et al.* (2010) Distinct Hematopoietic Stem Cell Subtypes Are Differentially Regulated by TGFβ1. *Cell Stem Cell* 6, 265–278

13 Beerman, I. *et al.* (2010) Functionally distinct hematopoietic stem cells modulate hematopoietic lineage potential during aging by a mechanism of clonal expansion. *Proc. Natl. Acad. Sci. U. S. A.* 107, 5465–5470

14 Sawai, C.M. *et al.* (2016) Hematopoietic Stem Cells Are the Major Source of Multilineage Hematopoiesis in Adult Animals. *Immunity* 45, 597–609

15 Pei, W. *et al.* (2020) Resolving Fates and Single-Cell Transcriptomes of Hematopoietic Stem Cell Clones by PolyloxExpress Barcoding. *Cell Stem Cell* 27, 383-395.e8

16 Rodriguez-Fraticelli, A.E. *et al.* (2020) Single-cell lineage tracing unveils a role for TCF15 in haematopoiesis. *Nature* 583, 585–589

17 Bowling, S. *et al.* (2020) An Engineered CRISPR-Cas9 Mouse Line for Simultaneous Readout of Lineage Histories and Gene Expression Profiles in Single Cells. *Cell* 181, 1410-1422.e27

18 Sun, J. *et al.* (2014) Clonal dynamics of native haematopoiesis. *Nature* 514, 322–327

19 Abkowitz, J.L. *et al.* (2002) Evidence that the number of hematopoietic stem cells per animal is conserved in mammals. *Blood* 100, 2665–2667

20 Lee-Six, H. *et al.* (2018) Population dynamics of normal human blood inferred from somatic mutations. *Nature* 561, 473–478

21 Watson, C.J. *et al.* (2020) The evolutionary dynamics and fitness landscape of clonal hematopoiesis. *Science* 367, 1449–1454

22 Biasco, L. *et al.* (2016) In Vivo Tracking of Human Hematopoiesis Reveals Patterns of Clonal Dynamics during Early and Steady-State Reconstitution Phases. *Cell Stem Cell* 19, 107–119

23 Sommerkamp, P. *et al.* (2021) Mouse multipotent progenitor 5 cells are located at the interphase between hematopoietic stem and progenitor cells. *Blood* 137, 3218–3224

24 Morrison, S.J. and Weissman, I.L. (1994) The long-term repopulating subset of hematopoietic stem cells is deterministic and isolatable by phenotype. *Immunity* 1, 661–673

25 Morrison, S.J. *et al.* (1997) Identification of a lineage of multipotent hematopoietic progenitors. *Dev. Camb. Engl.* 124, 1929–1939

26 Akashi, K. *et al.* (2000) A clonogenic common myeloid progenitor that gives rise to all myeloid lineages. *Nature* 404, 193–197

27 Nakorn, T.N. *et al.* (2003) Characterization of mouse clonogenic megakaryocyte progenitors. *Proc. Natl. Acad. Sci.* 100, 205–210

28 Harman, B.C. *et al.* (2008) Resolution of Unique Sca-1 ^{high} c-Kit $^{-}$ Lymphoid-Biased Progenitors in Adult Bone Marrow. *J. Immunol.* 181, 7514–7524

29 Kumar, R. *et al.* (2008) Lin−Sca1+Kit− Bone Marrow Cells Contain Early Lymphoid-Committed Precursors That Are Distinct from Common Lymphoid Progenitors. *J. Immunol.* 181, 7507–7513

30 Giandomenico, S.D. *et al.* (2019) Megakaryocyte TGFβ1 Partitions Hematopoiesis into Immature Progenitor/Stem Cells and Maturing Precursors. *bioRxiv* DOI: 10.1101/689901

31 Kirby, M.R. and Donahue, R.E. (1993) Rare Event Sorting of CD34+ Hematopoietic Cells. *Ann. N. Y. Acad. Sci.* 677, 413–416

32 Hao, Q.-L. *et al.* (1995) A Functional Comparison of CD34+ CD38– Cells in Cord Blood and Bone Marrow. *Blood* 86, 3745–3753

33 Farrell, T. *et al.* (2014) Changes in the frequencies of human hematopoietic stem and progenitor cells with age and site. *Exp. Hematol.* 42, 146–154

34 Povsic, T.J. *et al.* (2010) Aging is not associated with bone marrow-resident progenitor cell depletion. *J. Gerontol. A. Biol. Sci. Med. Sci.* 65, 1042–1050

35 Boyer, S.W. *et al.* (2019) Clonal and Quantitative In Vivo Assessment of Hematopoietic Stem Cell Differentiation Reveals Strong Erythroid Potential of Multipotent Cells. *Stem Cell Rep.* 12, 801–815

36 Niswander, L.M. *et al.* (2014) Improved quantitative analysis of primary bone marrow megakaryocytes utilizing imaging flow cytometry. *Cytometry A* 85, 302–312

37 Basilico, S. and Göttgens, B. (2017) Dysregulation of haematopoietic stem cell regulatory programs in acute myeloid leukaemia. *J. Mol. Med. Berl. Ger.* 95, 719–727

38 Krueger, A. *et al.* (2017) T Cell Development by the Numbers. *Trends Immunol.* 38, 128–139

39 Romar, G.A. *et al.* (2016) Research Techniques Made Simple: Techniques to Assess Cell Proliferation. *J. Invest. Dermatol.* 136, e1–e7

40 Wilson, A. *et al.* (2008) Hematopoietic stem cells reversibly switch from dormancy to self-renewal during homeostasis and repair. *Cell* 135, 1118–1129

41 Akinduro, O. *et al.* (2018) Proliferation dynamics of acute myeloid leukaemia and haematopoietic progenitors competing for bone marrow space. *Nat. Commun.* 9, 519

42 Takahashi, M. *et al.* (2021) Reconciling Flux Experiments for Quantitative Modeling of Normal and Malignant Hematopoietic Stem/Progenitor Dynamics. *Stem Cell Rep.* 16, 741–753

43 Signer, R.A.J. *et al.* (2016) The rate of protein synthesis in hematopoietic stem cells is limited partly by 4E-BPs. *Genes Dev.* 30, 1698–1703

44 Catlin, S.N. *et al.* (2011) The replication rate of human hematopoietic stem cells in vivo. *Blood* 117, 4460–4466

45 Borghans, J.A.M. *et al.* (2018) Current best estimates for the average lifespans of mouse and human leukocytes: reviewing two decades of deuterium-labeling experiments. *Immunol. Rev.* 285, 233–248

46 Ballesteros, I. *et al.* (2020) Co-option of Neutrophil Fates by Tissue Environments. *Cell* 183, 1282-1297.e18

47 Verheijen, M. *et al.* (2020) Fate Mapping Quantifies the Dynamics of B Cell Development and Activation throughout Life. *Cell Rep.* 33,

48 Bernitz, J.M. *et al.* (2016) Hematopoietic Stem Cells Count and Remember Self-Renewal Divisions. *Cell* 167, 1296-1309.e10

49 Chambers, S.M. *et al.* (2007) Aging hematopoietic stem cells decline in function and exhibit epigenetic dysregulation. *PLoS Biol.* 5, e201

50 Harker, L.A. and Finch, C.A. (1969) Thrombokinetics in man. *J. Clin. Invest.* 48, 963–974

51 Amann-Zalcenstein, D. *et al.* (2020) A new lymphoid-primed progenitor marked by Dach1 downregulation identified with single cell multi-omics. *Nat. Immunol.* 21, 1574–1584

52 Model, M.A. (2018) Methods for cell volume measurement. *Cytometry A* 93, 281–296

53 Hidalgo San Jose, L. *et al.* (2020) Modest Declines in Proteome Quality Impair Hematopoietic Stem Cell Self-Renewal. *Cell Rep.* 30, 69-80.e6

54 Signer, R.A.J. *et al.* (2014) Haematopoietic stem cells require a highly regulated protein synthesis rate. *Nature* 509, 49–54

55 Agathocleous, M. *et al.* (2017) Ascorbate regulates haematopoietic stem cell function and leukaemogenesis. *Nature* 549, 476–481

56 Leidl, K. *et al.* (2008) Mass spectrometric analysis of lipid species of human circulating blood cells. *Biochim. Biophys. Acta BBA - Mol. Cell Biol. Lipids* 1781, 655–664

57 Radley, J.M. *et al.* (1999) Ultrastructure of primitive hematopoietic stem cells isolated using probes of functional status. *Exp. Hematol.* 27, 365–369

58 Noris, P. *et al.* (2014) Platelet diameters in inherited thrombocytopenias: analysis of 376 patients with all known disorders. *Blood* 124, e4–e10

59 H, D. *et al.* (2011) Normal range of mean platelet volume in healthy subjects: Insight from a large epidemiologic study. *Thromb. Res.* 128,

60 Bessman, J.D. (1984) The relation of megakaryocyte ploidy to platelet volume. *Am. J. Hematol.* 16, 161–170

61 Mclaren, C.E. *et al.* (1987) Statistical and graphical evaluation of erythrocyte volume distributions. *Am. J. Physiol. 252 Heart Circ. Physiol.*

62 Downey, G.P. *et al.* (1990) Retention of leukocytes in capillaries: role of cell size and deformability. *J. Appl. Physiol. Bethesda Md 1985* 69, 1767–1778

63 Ting-Beall, H.P. *et al.* (1993) Volume and osmotic properties of human neutrophils. *Blood* 81, 2774–2780

64 Needham, D. and Hochmuth, R.M. (1990) Rapid flow of passive neutrophils into a 4 microns pipet and measurement of cytoplasmic viscosity. *J. Biomech. Eng.* 112, 269–276

65 Kuse, R. *et al.* (1985) Blood lymphocyte volumes and diameters in patients with chronic lymphocytic leukemia and normal controls. *Blut* 50, 243–248

66 Chervenick, P.A. *et al.* (1968) Quantitative studies of blood and bone marrow neutrophils in normal mice. *Am. J. Physiol.* 215, 353–360

67 Méndez-Ferrer, S. *et al.* (2010) Mesenchymal and haematopoietic stem cells form a unique bone marrow niche. *Nature* 466, 829–834

68 Worthley, D.L. *et al.* (2015) Gremlin 1 Identifies a Skeletal Stem Cell with Bone, Cartilage, and Reticular Stromal Potential. *Cell* 160, 269–284

69 Zhou, B.O. *et al.* (2014) Leptin-Receptor-Expressing Mesenchymal Stromal Cells Represent the Main Source of Bone Formed by Adult Bone Marrow. *Cell Stem Cell* 15, 154–168

70 Gomariz, A. *et al.* (2018) Quantitative spatial analysis of haematopoiesis-regulating stromal cells in the bone marrow microenvironment by 3D microscopy. *Nat. Commun.* 9, 2532

71 Menees, K.B. *et al.* (2021) Sex- and age-dependent alterations of splenic immune cell profile and NK cell phenotypes and function in C57BL/6J mice. *Immun. Ageing* 18, 3

72 Kaliss, N. and Pressman, D. (2016) Plasma and Blood Volumes of Mouse Organs, As Determined with Radioactive Iodoproteins.∗: *Proc. Soc. Exp. Biol. Med.* DOI: 10.3181/00379727-75-18083

73 Furth, J. and Sobel, H. (1946) Hypervolemia Secondary to Grafted Granulosa-Cell Tumor2. *JNCI J. Natl. Cancer Inst.* 7, 103–113

74 Keighley, G. *et al.* (1962) Response of Normal and Genetically Anaemic Mice to Erythropoietic Stimuli*. *Br. J. Haematol.* 8, 429–441

75 Riches, A.C. *et al.* (1973) Blood volume determination in the mouse. *J. Physiol.* 228, 279–284

76 Sluiter, W. *et al.* (1984) Determination of blood volume in the mouse with 51Chromium-labelled erythrocytes. *J. Immunol. Methods* 73, 221–225

77 Van den Broeck, W. *et al.* (2006) Anatomy and nomenclature of murine lymph nodes: Descriptive study and nomenclatory standardization in BALB/cAnNCrl mice. *J. Immunol. Methods* 312, 12–19

78 Kawashima, Y. *et al.* (1964) The lymph system in mice. *Subj. Strain Bibliogr. 1964*

79 Druzd, D. *et al.* (2017) Lymphocyte Circadian Clocks Control Lymph Node Trafficking and Adaptive Immune Responses. *Immunity* 46, 120–132

80 Hsu, H.-C. *et al.* (2003) Age-related thymic involution in C57BL/6J × DBA/2J recombinant-inbred mice maps to mouse chromosomes 9 and 10. *Genes Immun.* 4, 402–410

81 Allman, D.M. *et al.* (1993) Peripheral B cell maturation. II. Heat-stable antigen(hi) splenic B cells are an immature developmental intermediate in the production of long-lived marrow-derived B cells. *J. Immunol. Baltim. Md 1950* 151, 4431–4444

82 Kaufman, R.M. *et al.* (1965) Circulating megakaryocytes and platelet release in the lung. *Blood* 26, 720–731

83 Trowbridge, E.A. *et al.* (1984) The origin of platelet count and volume. *Clin. Phys. Physiol. Meas. Off. J. Hosp. Phys. Assoc. Dtsch. Ges. Med. Phys. Eur. Fed. Organ. Med. Phys.* 5, 145–170

84 Buttgereit, F. and Brand, M.D. (1995) A hierarchy of ATP-consuming processes in mammalian cells. *Biochem. J.* 312, 163–167
85 Argüello, R.J. *et al.* (2020) SCENITH: A Flow Cytometry-Based Method to Functionally Profile Energy Metabolism with Single-Cell Resolution. *Cell Metab.* 32, 1063-1075.e7
86 Brocchieri, L. and Karlin, S. (2005) Protein length in eukaryotic and prokaryotic proteomes. *Nucleic Acids Res.* 33, 3390–3400
87 Sarpel, G. *et al.* (1982) Erythrocyte phosphate content in Huntington's disease. *Neurosci. Lett.* 31, 91–96
88 Thore, A. *et al.* (1975) Detection of bacteriuria by luciferase assay of adenosine triphosphate. *J. Clin. Microbiol.* 1, 1–8
89 Lew, V.L. and Tiffert, T. (2017) On the Mechanism of Human Red Blood Cell Longevity: Roles of Calcium, the Sodium Pump, PIEZO1, and Gardos Channels. *Front. Physiol.* 8, 977
90 Müller, E. *et al.* (1986) Turnover of phosphomonoester groups and compartmentation of polyphosphoinositides in human erythrocytes. *Biochem. J.* 235, 775–783
91 Feig, S.A. *et al.* (1972) Energy metabolism in human erythrocytes. *J. Clin. Invest.* 51, 1547–1554
92 Child, J.A. *et al.* (1967) A diffraction method for measuring the average volumes and shapes of red blood cells. *Br. J. Haematol.* 13, 364–375
93 van Meer, G. *et al.* (2008) Membrane lipids: where they are and how they behave. *Nat. Rev. Mol. Cell Biol.* 9, 112–124
94 Bogue, M.A. *et al.* (2020) Mouse Phenome Database: a data repository and analysis suite for curated primary mouse phenotype data. *Nucleic Acids Res.* 48, D716–D723
95 Kawashima, Y. *et al.* (1964) THE LYMPH SYSTEM IN MICE.
96 Druzd, D. *et al.* (2017) Lymphocyte Circadian Clocks Control Lymph Node Trafficking and Adaptive Immune Responses. *Immunity* 0,
97 Tanaka, S. *et al.* (2020) Tet2 and Tet3 in B cells are required to repress CD86 and prevent autoimmunity. *Nat. Immunol.* 21, 950–961

Figure Legends

Figure 1: Generating reference values for total murine hematopoietic cell numbers. Most studies enumerate cell frequency by measuring a tissue sample. Consequently, these value needs to be transformed to absolute count, scaled up to the entire organism and corrected for sampling and technical artefacts. All the numbers are derived for a reference adult female mouse of 12 weeks weighing 22g. For total cell numbers in blood, we summed the total numbers of leukocytes, platelets and erythrocytes per μl and multiply this by the total blood volume for our reference mouse. In the bone marrow, we scale the measurement of the number of nucleated cells per gram of body weight of a 22g reference mouse and then we add to this number the proportion of anucleated erythrocytes and platelets. For the thymus, the total number of thymocytes at birth is corrected for the loss of thymocytes associated with ageing using the rate of thymocyte loss per day for a 12 weeks old reference mouse. For the lymph node, the number of cells within one lymph node is multiplied by the average total number of lymph nodes in 1 mouse. For the spleen, we take a measurement of the total splenocytes per gram of spleen and then scale it by the mass of the spleen in our reference mouse. A full

557 explanation of these calculations, along with supporting references, is provided in file S1 and
558 S2.
559
560
561 **Figure 2: Cell numbers across different hematopoietic compartments in healthy mice** (A)
562 Calculated total number of cells across the murine hematopoietic hierarchy using values in
563 Table 1. To help understand the scaling across several orders of magnitude, we place
564 compartment sizes on a more familiar scale: time. Specifically, we place cells on a time scale
565 where 1 cell is arbitrarily equal to 1 second. All the numbers are derived for a reference adult
566 female mouse of 12 weeks weighing 22g (Table 1). HSC = hematopoietic stem cells, MPP =
567 multi-potent progenitors, RPP = restricted potential progenitor, RBC = red blood cell.
568

569 **Figure 3. The dynamics of steady-state murine hematopoiesis.** Calculating the minimum
570 division number between active HSCs and mature cell subsets for red blood cells and myeloid
571 cells (A). This minimum division number is computed with the logarithmic 2 transformation
572 of total cell numbers in the body of a certain cell type (N_{mature}) divided by the number of active
573 hematopoietic stem cells (N_{hsc}). This calculation does not consider the impact of cell death and
574 differentiation. (B) For B cells, positive and negative selection of mature naïve B cells was
575 considered and (C) for megakaryocytes, endomitosis has also been accounted for, (D) as well
576 as platelets fragmentation. (D) Summary of the values for the reference mice, as in file S1. (E)
577 Estimating the turnover rates of the blood cell lineages, assuming that production and death
578 rates balance in healthy young adult mice. In this scheme the number of cells produced each
579 day ($N_{cell\ produced}$) is the product of the total cell number (N_{cell}), the production rate and potential
580 selection (as for B cells) of each cell type per day (P(D)). (F) The calculated cell population
581 sizes in given organs, expected P(D) for each blood cell lineage during hematopoiesis for the
582 reference mouse, as in Table 2. Details of all these calculations are provided in file S2.
583

Mouse organ /Cell Population /	Value	Unit	Reference
Reference mouse			
Weight	22	g	[94]
Strain	B6		
Age	84	days	
Sex	female		
Bone Marrow			
Total cell count	4.5E+08	cells	[29,35,66]
Total nucleated cells	2.6E+08	cells	[66]
Lin^- cells	2.0E+07	cells	[10]
Phenotypic HSC[a] ($Lin^-Kit^+Sca\text{-}1^+CD150^+CD48^-$)	1.6E+04	cells	[10]
Active HSC	5.2E+03	cells	[10]
MPP[b] (non HSC LSK)	1.4E+05	cells	[10]
Erythro-myeloid progenitors	1.7E+06	cells	
CMP[c] ($Lin\text{-}Kit^+$ $CD16/32^-$ $CD34^+$)	4.0E+05	cells	[10]
GMP[d] ($Lin\text{-}Kit^+$ $CD16/32^+$ $CD34^+$)	5.1E+05	cells	[10]

MEP^{e} (Lin-Kit^{+} CD16/32^{-} CD34^{-})	8.0E+05	cells	[10]
Megakaryocyte progenitors	2.6E+04	cells	[27]
CLP	2.5E+05	cells	[10]
Lin^{+} cells	4.3E+08	cells	
Erythrocytes	1.8E+08	cells	[35]
Megakaryocytes	7.7E+05	cells	[36]
Platelets	5.6E+06	cells	[35]
Granulomyeloid	1.5E+08	cells	[35]
B cells	8.6E+07	cells	[35]
Peripheral Blood			
Volume	1.5E+03	ul	[76]
Total cell count	1.6E+10	cells	
Erythrocytes	1.5E+10	cells	[35]
Platelets	1.4E+09	cells	[35]
Granulomyeloid	1.7E+06	cells	[35]
B cells	8.3E+06	cells	[35]
T cells	2.6E+03	cells	[35]
Spleen			
Mass	7.9E-02	g	[71]
Total cell count	2.1E+08	cells	
Erythrocytes	8.2E+07	cells	[35]
Platelets	5.1E+07	cells	[35]
Granulomyeloid	2.7E+06	cells	[35]
B cells	4.7E+07	cells	[35]
Follicular Mature B cells	3.3E+07	cells	[35]
T cells	2.0E+07	cells	[35]
Lymph nodes			
Average number lymph nodes in whole body	2.7E+01	lymph nodes	[77,95]
Total cell count	7.6E+07	cells	[96]
Erythrocytes	2.5E+06	cells	[35]
B cells	3.5E+07	cells	[35]
Follicular Mature B cells	2.4E+07	cells	[97]
T cells	3.6E+07	cells	[35]
Others	1.5E+06	cells	[35]
Thymus			
Total cell count	2.1E+08	cells	[80]
Erythrocytes	3.6E+07	cells	[35]
Platelets	2.8E+06	cells	[35]

B cells	8.5E+06	cells	[35]
T cells	1.6E+08	cells	[35]

Table 1: Cellular composition of the main hematopoietic organs in our reference mouse, 16 weeks old female C57BL/6J weighing 22g. according to calculations in Box 1. HSC: hematopoietic stem cell ; MPP: multipotent progenitor ; CMP: common myeloid progenitor ; GMP: granulocyte-monocyte progenitor ; MEP: Megakaryocyte- erythroid progenitor. a = $Lin^-Kit^+Sca\text{-}1^+CD150^+CD48^-$; b = $Lin^-Kit^+Sca\text{-}1^+CD48^+$, c = $Lin\text{-}Kit^+$ $CD16/32^-$ $CD34^+$, d = $Lin\text{-}Kit^+$ $CD16/32^+$ $CD34^+$, e = $Lin\text{-}Kit^+$ $CD16/32^-$ $CD34^-$

Cell type	Organ	Cell count	Half-life (days)	Lifespan (days)*	Death Rate (/day)	Developmental Selection Rate	Cells produced (/day)**	Cells produced (/year)**	References
Red blood cells	Blood	1.5E+10	24.3	**35.00**	0.03	-	4.5E+08	1.6E+11	[59]
Platelets	Blood	1.4E+09	2.5	**3.60**	0.28	-	3.9E+08	1.4E+11	[59] , [60]
Myeloid	BM	1.5E+08	**0.84**	1.21	0.83	-	1.2E+08	4.5E+10	[46]
B cells (Follicular Mature)	Spleen and LN	5.7E+07	24.3	**35.00**	0.03	**0.03**	5.6E+07	2.0E+10	[47,81]

Table 2. Total number and production rate of hematopoietic cells in our reference mouse. Cell counts come from Calculations S1a and Table S1. Half-lives or lifespans were retrieved from the given articles (as indicated in bold) and used to provide an insight of the mature hematopoietic cell population turnover using the following simple relationships: *Lifespan = 1/Death rate = $t_{1/2}/\ln(2)$ ** cells produced = death rate x time period in days x Developmental Selection rate x cell count.

Cell Type	Estimated Cell Count	Lifespan (days)	Cells produced per day	References
Red blood cells	2.5×10^{13} cells	116	2.1×10^{11}	[4]
Monocytes	5.0×10^{9}	3.5	1.5×10^{9}	[4]
Platelets	1.5×10^{12} cells	9.9	1.5×10^{11}	[50]
Neutrophils	6.4×10^{11}	6.6	6×10^{10}	[4]
Mature B cells	3.0×10^{11}	63	5×10^{9}	[4]
Mature T cells	7.0×10^{11}	323	2×10^{9}	[4]

Table 3. Total number and production rate of human hematopoietic cells for our reference person

608

609 **Glossary**

610

611

Term	Description
Multipotency	The potential to differentiate into diverse blood cell lineages
Self-renewal	Cell division with maintenance of an undifferentiated cell state
Differentiation active	A stem or progenitor cell that is in the process of changing into a more mature hematopoietic cell type
Fate mapping	Labelling cells with a heritable mark to understand developmental processes
Lineage tracing	Fate mapping carried out at single cell resolution, typically by introducing a genetic label
Limited dilution assay	A technique to estimate the frequency of functional hematopoietic stem cells within a heterogeneous starting cell population. In this method a serial dilution of the starting cell population is performed and each subpopulation is functionally assessed by transplantation into a conditioned recipient
Capture-recapture analyses	A technique to estimate population sizes when it is not possible to count each individual cell. The method involves taking a small population of cells and labelling them, then reintroducing labelled cells back into their initial environment and determining the ratio of marked to unmarked cells at a later timepoint.
Post-transplantation hematopoiesis	The formation of new blood cells from stem cells that have been injected into a conditioned (typically irradiated) host.
Lentiviral vector integration site	In gene therapy, a viral vector is used to introduce new genetic material into a host organism. As the integration of the virus is stochastic, the precise location of the new genetic material in the host genome acts as a genetic label to perform fate mapping.
Division-linked dilution assay	A dye that is split equally between daughter cells during cell division. Consequently, the amount of dye in each cell is indicative of how many times it has divided, over a small number of generations.
Restricted Potential Progenitor	A hematopoietic cell that gives rise to multiple cell types, but that is incapable of creating all hematopoietic lineages. These cells therefore have less potential than MPPs and HSCs.
Endomitoses	Chromosome replication in the absence of a cell division, resulting in a polypoidal cell.
Lineage negative	A cell which does not express surface markers associated with the mature blood cell lineages
Restricted-potential progenitor	Hematopoietic progenitors in the murine bone marrow, this population comprises CMPs, CLPs, GMPs, MEPs, MkPs
$CD34^+$ progenitor	The human progenitor compartment containing HSCs, MPPs, and restricted-potential progenitors.
HSC	A Hematopoietic Stem Cell, functionally defined as a multipotent cell capable of long-term self-renewal. In this study we consider an immunophenotypic HSC to express the following pattern of markers: Lin^-Kit^+ $Sca\text{-}1^+CD150^+CD48^-$

MPP	A Multi-Potent Progenitor, functionally defined as a cell capable of producing all lineages, but lacking long-term self-renewal. In this study we consider that murine MPPs are all $Lin^{-}Kit^{+}$ $Sca\text{-}1^{+}$ cells that are not within the immunophenotypic HSC compartment
CMP	A Common Myeloid Progenitor that gives rise to the erythroid, megakaryocyte and myeloid lineages. In mice expresses the following markers: $cKit^{+}$ $Sca1^{-}$ $CD16/32^{-}$ $CD34^{+}$
MEP	A Megakaryocyte-Erythroid Progenitor that gives rise to erythroblasts and megakaryocytes. In mice expresses the following markers: $cKit^{+}$ $Sca1^{-}$ $CD16/32^{-}$ $CD34^{-}$
GMP	A Granulocytic-Monocytic Progenitor that gives rise to the myeloid lineages. In mice expresses the following markers: $cKit^{+}$ $Sca1^{-}$ $CD16/32^{+}$ $CD34^{+}$
CLP	A Common Lymphoid Progenitor that gives rise to B and T lymphocytes. In mice expresses the following markers: $cKit^{low}$ $Sca1^{low}$ $IL7R^{+}$ $Flk2^{-}$
MkP	A Megakarocyte progenitor. In mice expresses the following markers: $Sca1^{-}$ $FcyR^{low}$ $CD9^{+}$ $CD41^{+}$

612
613
614

615

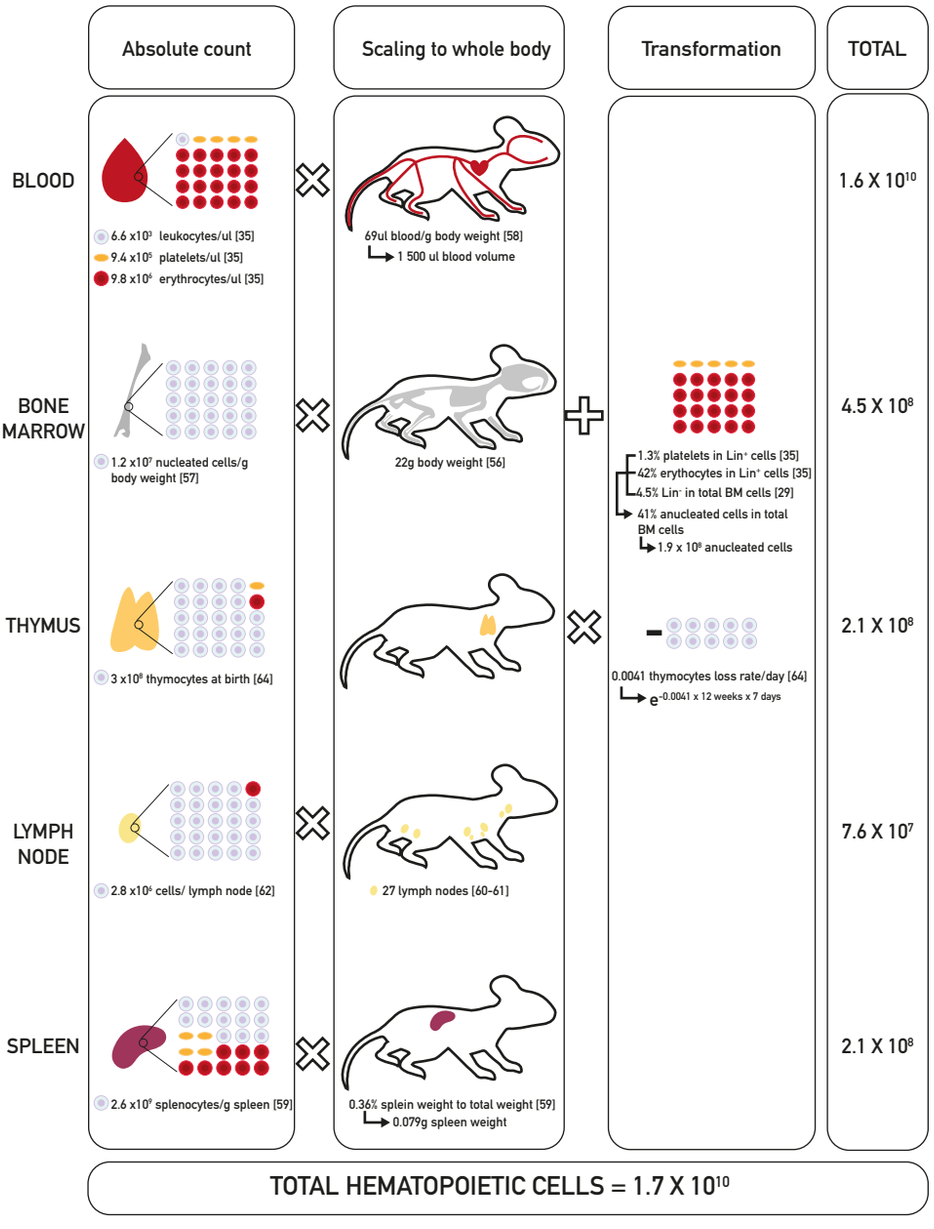
Absolute count
Scaling to whole body
Transformation
TOTAL
BLOOD
6.6 x10³ leukocytes/ul [35]
9.4 x10⁵ platelets/ul [35]
9.8 x10⁶ erythrocytes/ul [35]
69ul blood/g body weight [58]
1 500 ul blood volume
1.6 X 10¹⁰
BONE MARROW
1.2 x10⁷ nucleated cells/g body weight [57]
22g body weight [56]
1.3% platelets in Lin⁺ cells [35]
42% erythocytes in Lin⁺ cells [35]
4.5% Lin⁻ in total BM cells [29]
41% anucleated cells in total BM cells
1.9 x 10⁸ anucleated cells
4.5 X 10⁸
THYMUS
3 x10⁸ thymocytes at birth [64]
0.0041 thymocytes loss rate/day [64]
e-0.0041 x 12 weeks x 7 days
2.1 X 10⁸
LYMPH NODE
2.8 x10⁴ cells/ lymph node [62]
27 lymph nodes [60-61]
7.6 X 10⁷
SPLEEN
2.6 x10⁹ splenocytes/g spleen [59]
0.36% splein weight to total weight [59]
0.079g spleen weight
2.1 X 10⁸
TOTAL HEMATOPOIETIC CELLS = 1.7 X 10¹⁰

10^4 HSC
4 hours

10^5 MPP
39 hours

10^6 RPP
23 days

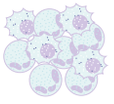

10^8 Granulomyeloids
5 years

10^9 Platelets
48 years

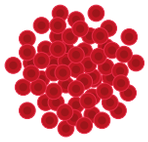

10^{10} Erythrocytes
476 years

10^8 Lymphoids
11 years

if 1 = *1second*

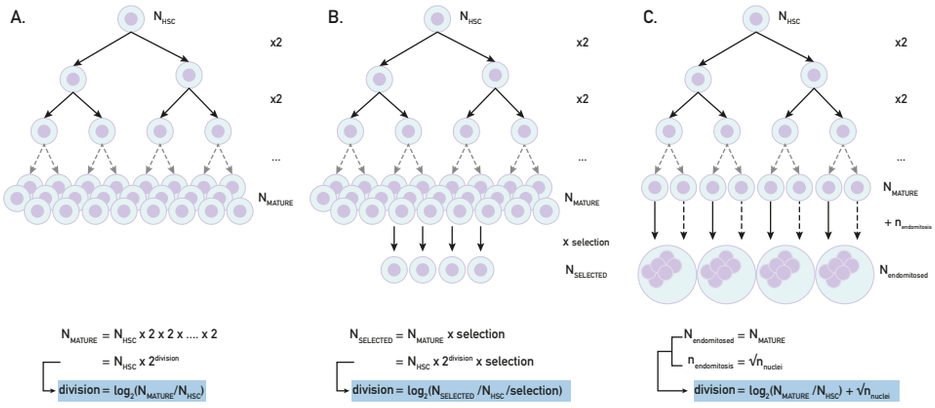
A.
N_{HSC}
x2
x2
...
N_{MATURE}
B.
N_{HSC}
x2
x2
...
N_{MATURE}
x selection
$N_{SELECTED}$
C.
N_{HSC}
x2
x2
...
N_{MATURE}
+ $n_{endomitosis}$
$N_{endomitosed}$
$N_{MATURE} = N_{HSC} \times 2 \times 2 \times .... \times 2$
$= N_{HSC} \times 2^{division}$
$division = \log_2(N_{MATURE}/N_{HSC})$
$N_{SELECTED} = N_{MATURE} \times selection$
$= N_{HSC} \times 2^{division} \times selection$
$division = \log_2(N_{SELECTED}/N_{HSC}/selection)$
$N_{endomitosed} = N_{MATURE}$
$n_{endomitosis} = \sqrt{n_{nuclei}}$
$division = \log_2(N_{MATURE}/N_{HSC}) + \sqrt{n_{nuclei}}$

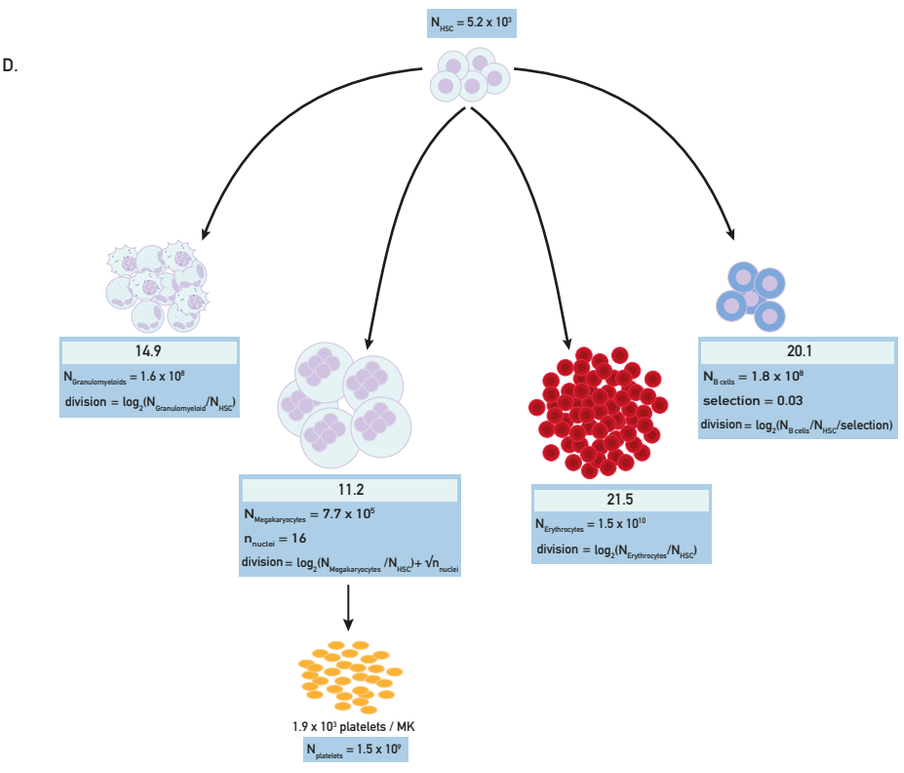
D.
$N_{HSC} = 5.2 \times 10^3$
14.9
$N_{Granulomyeloids} = 1.6 \times 10^8$
$division = \log_2(N_{Granulomyeloid}/N_{HSC})$
11.2
$N_{Megakaryocytes} = 7.7 \times 10^5$
$n_{nuclei} = 16$
$division = \log_2(N_{Megakaryocytes}/N_{HSC}) + \sqrt{n_{nuclei}}$
1.9 x 10^3 platelets / MK
$N_{platelets} = 1.5 \times 10^9$
21.5
$N_{Erythrocytes} = 1.5 \times 10^{10}$
$division = \log_2(N_{Erythrocytes}/N_{HSC})$
20.1
$N_{B\ cells} = 1.8 \times 10^8$
selection = 0.03
$division = \log_2(N_{B\ cells}/N_{HSC}/selection)$

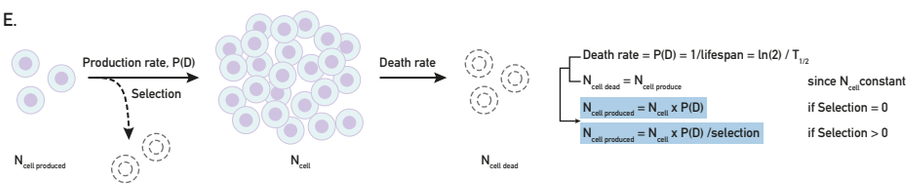
E.
Production rate, P(D)
Selection
$N_{cell\ produced}$
N_{cell}
Death rate
$N_{cell\ dead}$
Death rate = P(D) = 1/lifespan = ln(2) / $T_{1/2}$
$N_{cell\ dead} = N_{cell\ produce}$
$N_{cell\ produced} = N_{cell} \times P(D)$
$N_{cell\ produced} = N_{cell} \times P(D)$ /selection
since N_{cell} constant
if Selection = 0
if Selection > 0

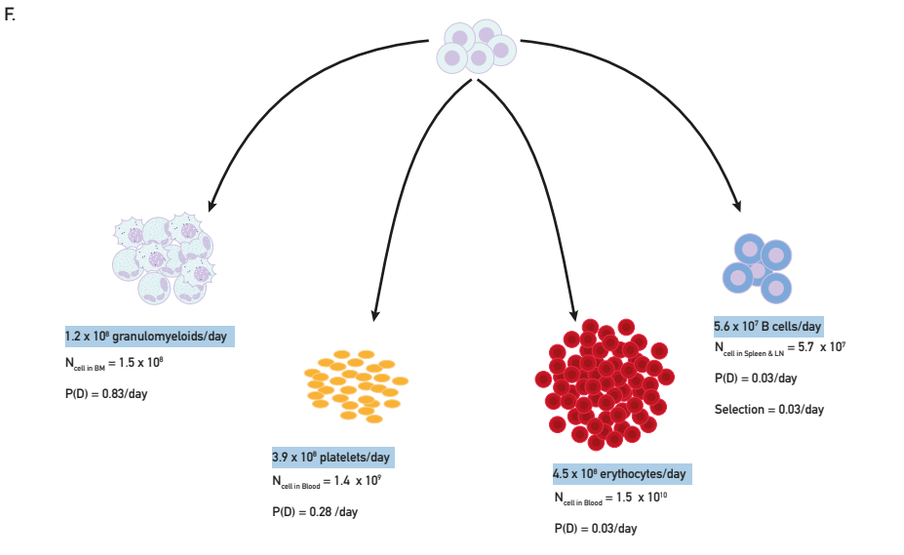
F.
1.2 x 10^8 granulomyeloids/day
$N_{cell\ in\ BM} = 1.5 \times 10^8$
P(D) = 0.83/day
3.9 x 10^8 platelets/day
$N_{cell\ in\ Blood} = 1.4 \times 10^9$
P(D) = 0.28 /day
4.5 x 10^8 erythocytes/day
$N_{cell\ in\ Blood} = 1.5 \times 10^{10}$
P(D) = 0.03/day
5.6 x 10^7 B cells/day
$N_{cell\ in\ Spleen\ \&\ LN} = 5.7 \times 10^7$
P(D) = 0.03/day
Selection = 0.03/day

File S2: Supplementary Material

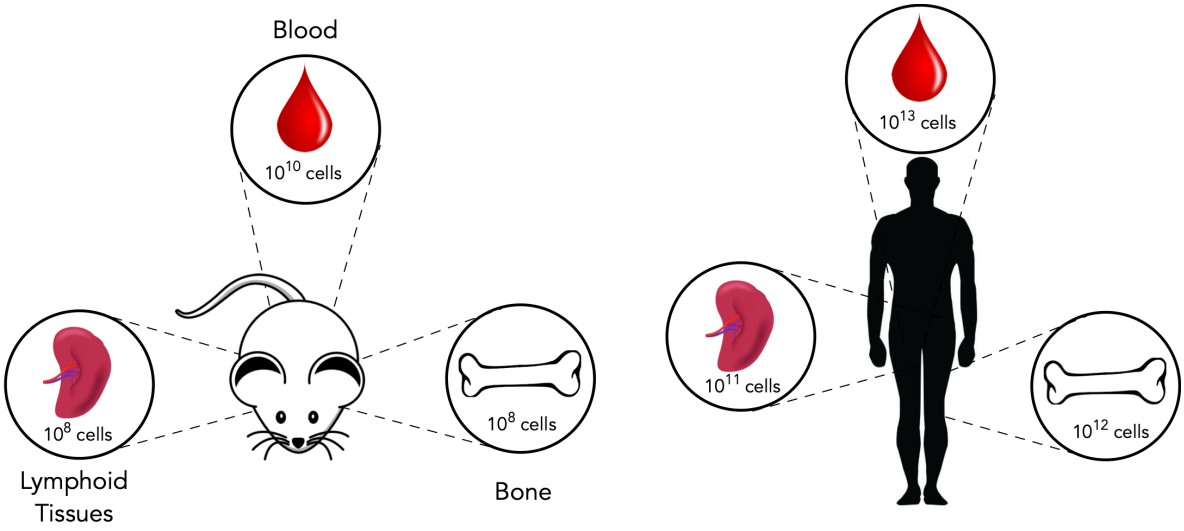

Figure S1. **Calculated cell numbers across different hematopoietic organs at steady state in mice and humans**(A) Calculated total number of cells in the peripheral blood, bone marrow, and lymphoid tissues (spleen, thymus and lymph nodes) of mice and humans.

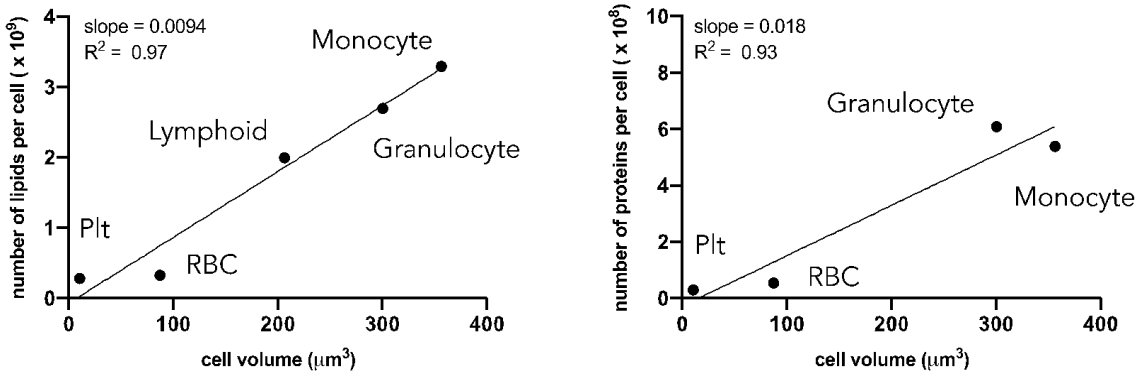

Figure S2. Linear models relating cell volume to absolute numbers of lipids and proteins in human mature hematopoietic cells taken from peripheral blood. Original data for this figure is derived from **[56]** and is presented in full in file S1. On the right-hand side, only the erythromyeloid lineages are plotted. The measured protein content of the lymphoid lineage was much higher than the erythromyeloid lineages, and so the Bichinchoninic Acid Assay measurements of lymphoid protein content (**data provided in table 4**) cannot be explained by the linear trend relating cell size to protein content for the erythromyeloid lineages. Plt: platelet ; RBC: red blood cells.

Cell Type	Diameter (μm)	Volume (μm^3)	Lipids/cell (x 10^9)	Proteins/cell (x 10^8)	Data Source	References
HSC	7*	175	unknown	unknown	Mice	[53], [57]
Platelet	2.6	9.1	0.3	0.3	Human	[56], [58–60]
RBC	7.7	88	0.3	0.6	Human	[56], [61],
Granulocyte	8.4	290	2.7	6.1	Human	[56],[62],[63][64]
Monocyte	8.8	357**	3.3	5.4	Human	[56],[62]
Lymphocyte	7	208	2	9.5	Human	[56], [65],[62]

Table S1. Distribution of cell volumes and macromolecular content across different human compartments. * data taken from mice. **estimated by modelling cell shape as a sphere**.** Protein and lipid content of human blood cells measured using a Bichinchoninic Acid Assay and Electrospray Ionization Mass-Spectrometry respectively **[56]**. A full derivation of protein and lipid numbers is provided in calculation S2h-i.

77

Sources and criteria for numbers used in our calculations:

In this supplementary section we perform calculations to contextualize key numbers in hematopoiesis and provide directions for future research. The sources and criteria used for the numbers included in this section, along with associated metadata can be found in **file S1**.

Where appropriate we specify whether the calculations refer to human or murine hematopoiesis. Final values are considered representative of either a female mouse aged 12 weeks and weighing 22grams or a 20-30 human male weighing 70kg. Please note that all measurements have been rounded to one digital for the calculations.

The final values obtained from our calculations are also rounded to one decimal place but that rounding of numbers is not performed at intermediate calculation steps. The results of the intermediate steps are only made to help the reader to follow.

Calculation S1. How many hematopoietic cells are there?

Calculation 1a: What are the total number of hematopoietic cells across different tissues of a 22g adult female mouse?

Bone marrow

While current studies focus primarily on quantifying the absolute count of cells recovered from a given bone after flushing or crushing, this is not sufficient to infer the total number of bone marrow nucleated cells. Indeed, in order to quantify the total number of bone marrow nucleated cells, the distribution of bone marrow cells amongst all bones is essential to know, as well as the percentage of bone marrow cells recovered by flushing or crushing. Such numbers were quantified in studies using ^{59}Fe injection and radiation measurement of each bone of the murine skeleton [66], with the assumption that every bone contains a similar percentage of marrow erythropoietic tissue [66]. This assumption is supported by measurements obtained using radioactively labelled iron to estimate the erythroid content of bone marrow from different anatomical sites[66]. It is also important to note that the major hematopoietic organs contain non-hematopoietic stromal cells. In bone marrow, this cell

population represents about 1.5% of the entire nucleated cell compartment [67–69], however there can be significant variation in the proportions of stromal cells recovered depending on how the tissue was processed, [70]. Due to large variability in estimates of stromal cell frequencies, and their low abundance in the major hematopoietic organs (around 1%), which would not influence the order of magnitude of our estimate, they are not considered in our calculations. Accounting for the key factors detailed above, we estimate the total amount of nucleated bone marrow cells in the following manner:

Number of nucleated bone marrow cells/mouse body weight(g) x mouse body weight(g)

$$1.2\ x\ 10^7\ \frac{cells}{g} x\ 22g\ \approx 2.6\ \times\ 10^8\ nucleated\ cells$$

However, these measurements only assess nucleated cells. Based on the Boyer et al measurements of the percentage of Ter119+ RBC (42%) and Cd61+ Platelets (1.3%) amongst mature cell lineages [28–30] (Lin+ cells) and the percentage of Lin^- cells of whole bone marrow cells (4.5%)[29], we can also derive the total number of hematopoietic cells in the bone marrow in the following manner:

Assuming,

Total BM cells = Nucleated cells / %nucleated cells in BM

Total BM cells = Nucleated cells + Anucleated cells

Then,

%nucleated cells in BM = 1 - %anucleated cells in BM = 1- (%RBC in BM+%platelets in BM)

And,

%RBC in BM = %RBC in Lin^+x %Lin^+in BM= %RBC in Lin^+x (1-%Lin^- in BM)

%platelets in BM = %platelets in Lin^+x %Lin^+in BM= %platelets in Lin^+x (1-%Lin^- in BM)

Therefore,

➔ *%nucleated cells in BM = 1-[(%RBC in Lin^++%platelets in Lin^+) x (1-%Lin^- in BM)]*

➔ *Total BM cells = Nucleated cells/[1-[(%RBC in Lin^++%platelets in Lin^+) x (1-%Lin^- in BM)]]*

$$\frac{2.6\ \times\ 10^8\ cells}{1-[(42\%+1.3\%)\times(1-4.5\%)]} \approx 4.5\ \times\ 10^8\ total\ bone\ marrow\ cells$$

Spleen

The spleen is known to be primarily constituted of hematopoietic cells to the extent that changes in spleen weight are regularly used as a biological readout for changes in hematopoietic cell numbers. However, quantifying the number of hematopoietic cells present in the spleen received little attention. We therefore took the approach to relate spleen weigh to spleen cellularity using data from [71] in the following manner:

Assuming,

Total spleen cells = number of splenocytes per gram of spleen x spleen weight (g)

Spleen weight = % spleen weight to total body weight x mouse weight (in grams)

Then,

Total spleen cells = number of splenocytes per gram of spleen x spleen weight

spleen weight to total body weight x mouse weight (in grams)

$$0.36\% \times 22g \times 2.6 \times 10^9 \frac{cells}{g} \approx 2.1 \times 10^8 \; cells$$

Peripheral Blood

Estimating the blood cellular content of our reference mouse is non-trivial. While immune cells frequencies in blood are one of the most robust measurements available, quantifying the total blood volume of a mouse is surprisingly challenging and has been disputed for almost a century. The main approach used in published papers is based on the concept that by measuring the dilution of a known component injected in blood, e.g. dye, radioactively labelled proteins or erythrocytes, it is possible to quantify back the total blood volume. However relatively strong experimental biases exist depending on whether the label is diluted in plasma (die or radioactive albumin) or in erythrocytes with values ranging from 29µl/g to 120µl/g body weight for various mouse strains [72–76]. In order to stay as closed to our reference mouse (adult female B6 mouse) and to use the most robust data, we decided to use Sluiter *et al.* blood volume measurement (69µl/g body weight), where a true regression line was inferred from data between blood volume and body weight [76]. Using this value along with cell counts/ul blood from Boyer *et al*, we computed the number of hematopoietic cells in the blood as 1.6 x 10^{10} cells using the following formula:

*(Granulomyeloids + platelets + RBC + B cells + T cells)(count/*µl*) x blood volume/body weight* (µl */g) x*

body weight (grams)

$$(1.1 \times 10^3 + 9.4 \times 10^5 + 9.8 \times 10^6 + 5.5 \times 10^3 + 1.7) \frac{cell}{\mu l} \times 69 \frac{\mu l}{g} \times 22g \approx 1.6 \times 10^{10} \; cells$$

Lymph Nodes

In the literature we find that each mouse has 22 – 32 lymph nodes [77,78] (i.e. an average of 27 lymph nodes and that each lymph node contains 1.5-4 million cells [79] (i.e., an average of 2.8 x 10^6 cells). Lymph nodes are difficult to distinguish from the surrounding fat and connective tissue, and so to count all of them lymph nodes were stimulated with adjuvant (activated lymph nodes become enlarged), and colored in vivo by an injection of Indian ink prior to dissection. Lymph node cellularity was measured by flow cytometry but this number is probably an underestimate of the true cellularity, as no quantification beads were used to correct for the volume of liquid recorded by the cytometer:

Number of cells per lymph node (cells) x total numbers of lymph nodes (lymph nodes per mouse)

$$2.8\ x\ 10^6 \frac{cells}{lymph\ node}\ x\ 27\ lymph\ nodes \approx 7.6 \times 10^7\ cells$$

Thymus

The thymus is known to decrease in size and cellular content over time in a process called thymic involution. In order to infer the amount of thymocytes present in our mouse model, we used the relationship between thymocytes count and female B6J mouse quantified by Hsu *et* al using a negative exponential curve[80]. Assuming our reference mouse is an adult of 12 weeks (84 days) we obtain the following estimate:

thymocyte counts at birth x exp(-thymocyte loss rate per day x mouse age in days)

$$3.0 \times 10^8\ thymocytes \times\ e^{-0.0041/day\ x\ 84\ days} \approx 2.1 \times 10^8\ cells$$

Calculation 1b: What are the relative numbers of hematopoietic progenitors in mice?

Before estimating the relative amounts of progenitor populations, we first derive the total number of HSCs in our reference mouse. Flow cytometry analyses from Busch *et al.* suggest that murine HSCs (Lin-Kit+ Sca-1+CD150+CD48-) represent 0.006% of all nucleated bone marrow cells [10] while our calculation in section S1a suggests there are 2.6 x 10^8 nucleated bone marrow cells. To estimate the total number of HSCs we perform the following calculation:

Number of bone marrow nucleated cells (cells) x HSC frequency (%)

$$(2.6 \times 10^8)\ cells \times\ 0.006\% \approx 16{,}000\ HSCs$$

Furthermore, Busch et al. also estimated that a minimum of 1 in 3 Tie2 induced YFP labelled HSC contribute actively to hematopoiesis. Assuming this characteristic can be extrapolated to all phenotypic HSCs this suggests, as reported by Busch et al, that our reference mice would have a minimum total number of HSCs of:

Number of HSC x minimum active HSC ratio

$$1.6 \times 10^4\ cells \times \frac{1}{3} \approx 5{,}200\ active\ HSCs$$

To calculate the sizes of the MPP CMP, GMP, MEP and CLP compartments we scale our reference value for HSCs by flow cytometry measurements of the relative compartment sizes [10] as follows

The MPP compartment is 9 times bigger than the HSC compartment

$$16{,}000 \times 9 = 1.4 \times 10^5$$

The CMP compartment is 2.9 times bigger than the MPP compartment

$$(1.4 \times 10^5) \times 2.9 = 4 \times 10^5$$

The GMP compartment is 3.6 times bigger than the MPP compartment

$$(1.4 \times 10^5) \times 3.6 = 5.1 \times 10^5$$

The MEP compartment is 5.7 times bigger than the MPP compartment

$$(1.4 \times 10^5) \times 5.7 = 8 \times 10^5$$

The CLP compartment is 1.8 times bigger than the MPP compartment

$$(1.4 \times 10^5) \times 1.8 = 2.5 \times 10^5$$

In this study megakaryocyte progenitors were not measured. To estimate the size of this compartment we use flow cytometry measurements of their frequency amongst all nucleated cells[27] and multiply this value by the total number of nucleated bone marrow cells:

Number of bone marrow nucleated cells (cells) x MkP frequency (%)

$$(2.6 \times 10^8) \times 0.01\% \approx 2.6 \times 10^4 MkPs$$

The MkP compartment is 0.2 times bigger than the MPP compartment

$$(1.4 \times 10^5) \times 0.2 = 2.6 \times 10^4$$

Summarising all of this data on a relative scale there are 9 MPPs per HSC, while one MPP will produce on average 2.9 CMPs, 3.6 GMPs, 5.7 MEPs , 0.2 MkP and 1.8 CLP

78

Calculation S2: The Dynamics and Bioenergetics of Hematopoiesis

Calculation 2a: the *minimum* number of divisions from HSC to myeloid and red blood cells in mice using only population sizes

To calculate the minimum number of divisions required to reach homeostatic cell numbers, we can use the fact that each division produce two cells and derive the number of divisions to produce a given number of mature cells assuming all stem cells contribute equally. This translates into the following equation:

$$N_{mature} = N_{hsc} \times 2^{division}$$

Where *division* is the number of generations it takes to reach steady state mature population sizes (in these calculations rounded to an order of magnitude approximation), not considering cell death and differentiation. N_{mature} and N_{hsc} represent the population sizes of the mature and HSC compartments. Using the number of mature cells and HSCs from the previous section, we can rearrange our formula and calculate minimal division requirements (*division)* for myeloid and red blood cells.

*Given that there are 5200 differentiation active HSCs, and that the mature myeloid and RBC compartments have $1.6x10^8$ and 1.5×10^{10} (**Table 1**) cells respectively (**as detailed in file S1**) we compute the following:*

HSC → M $\quad log_2(1.6 \times 10^8 \div 5200) \approx 14.9\ divisions$

HSC → RBC $\quad log_2(1.5 \times 10^{10} \div 5200) \approx 21.5\ divisions$

For B cells which undergo selection during development, and platelets which fragment from megakaryocytes, the number of divisions the dynamics are more complicated and are discussed in the subsequent sections.

Calculation 2b: the division number from HSC to naïve B cells in mice accounting for selection

A large proportion of B-cells generated do not reach the mature pool due to negative and positive selection. To estimate the effect of this selection, we combine the measurements from the same study of immature B cells produced from the bone marrow each day ($1.2x\ 10^7$ immature B cells) with the number of cells that enter the

mature naïve B-cell pool (0.6 x 10^6 mature naïve B cells per day)[81]. It suggests that 1 out of 20 immature B-cells will become a fully mature naive B cell. Of note, others have measured 0.9 x 10^6 mature naïve follicular mature (FM) B cells [47] but the measurement of immature B-cells is not available from the same study. Taking into account this selection factor, we calculate the number of divisions from HSC to naïve mature B cell by dividing the number of naïve B cells by the number of HSC. The number of naïve B cells is obtained by dividing total B-cell numbers ($1.4x10^8$, detailed in the main text) by our selection factor of 3%:

*Given that there are 5000 differentiation active HSCs, and $1.8x10^8$ B cells (**Table 1**) we compute the following:*

$$\text{HSC} \rightarrow \text{B} \qquad log_2(1.8 \times 10^8 \div 3\% \div 5200) \approx 20.1\ divisions$$

Calculation 2c: the minimum division from HSC to megakaryocyte in mice

Platelets are produced from progenitor cells called megakaryocytes. During maturation, megakaryocytes undergo endomitoses and accumulate a large amount of protein and membrane before fragmenting into platelets. Therefore, it is more appropriate to consider megakaryocyte numbers rather than platelet numbers for division numbers. Given that MKs represent 0.29% of nucleated bone marrow cells [36], there are around 8.1 x 10^5 megakaryocytes in the bone marrow of our reference mouse. For megakaryocytes this gives a minimal division requirement of:

*Given that there are 5200 differentiation active HSCs, and $8.1x10^5$ megakaryocytes (**as detailed in file S1**) we compute the following:*

$$\text{HSC} \rightarrow \text{Meg} \qquad log_2(7.7 \times 10^5 \div 5200) \approx 7.2\ divisions$$

Calculation 2d: Number of platelets produced per megakaryocyte in mice

Before giving rise to platelets megakaryocytes first undergo an additional 2-7 endomitoses. Given that most megakaryocytes are 16N [36], we assume that most megakaryocytes undergo 4 endomitoses. Summing the

minimal division number from HSC to Megakaryocytes (7.3 divisions as calculated above) with the 4 endomitoses, we get a total of 11.3 divisions/endomitoses. Given the number of platelets produced each day (**table 2**) and the total number of megakaryocytes (**table 1**), each megakaryocyte produces:

Platelets produced per day / number of megakaryocytes

$$4 \times 10^8 \div 7.7 \times 10^5 \approx 519\ platelets\ produced\ per\ megakaryocyte\ per\ day$$

Previously published estimates using the average megakaryocyte volume and the average platelet volume [82,83] or the daily platelet turnover rate in the blood and the total number of megakaryocytes [50] give similar values.

Calculation 2e: How many cells die each day per lineage in mice?

The number of cells that die each day per lineage can be calculated knowing the respective compartment sizes and half-lives. Compartment sizes and half-lives for our reference mouse reference are provided in Table S2, while the sources used in generating these reference values are provided in file S1. Using the following expression, we convert the half-life ($T_{1/2}$) into a death rate (P(D)) of each lineage to calculate how many cells die per day per lineage.

$$P(D) = \ln(2) / T_{1/2}$$

Multiplying this death rate P(D) by the total number of cells gives the number of cells that die each day (**Table S2**). As the death rate and production rates are equal at steady state, this value also represents daily bone marrow output:

$$\textbf{RBC} = 0.03 \times (1.5 \times 10^{10}) \approx 4.5 \times 10^8 cells\ per\ day$$

$$\textbf{Plt} = 0.28 \times (1.4 \times 10^9) \approx 3.9 \times 10^8 cells\ per\ day$$

$$\textbf{Myeloid} = 0.83 \times (1.5 \times 10^8) \approx 1.2 \times 10^8 cells\ per\ day$$

For B cells we must also take negative and positive selection into account. We therefore calculate the daily death rate as above:

$$\textbf{B cells} \;=\; 0.03 \;\times\; (5.7 \times 10^{7}) \approx 1.7 \;\times 10^{6} cells\ per\ day$$

and then divide this value by a selection factor which takes the number of immature B cells that enter the mature pool into account

$$3\% \;\div\; (1.7 \times 10^{6}) \approx 5.6 \;\times 10^{7}\ B\ cells\ produced\ per\ day$$

Calculation 2f: The protein synthesis requirements of erythromyeloid cell production in humans

Given our estimated turnover rates for myeloid cells and RBCs in humans (**table 3**), along with the total protein content of each cell type (**table S1**) we can compute the protein cost of cell production for each lineage.

Protein synthesis requirements = Number of cells produced per day x number of proteins per cell

$$\textbf{RBC} = (2.1 \times 10^{11}) \times (6 \times 10^{7}) \approx 1.3 \;\times 10^{19}\ proteins\ per\ day$$

$$\textbf{M} = (6.2 \times 10^{10}) \times (5.8 \times 10^{8}) \approx 3.6 \times 10^{19}\ proteins\ per\ day$$

These differences have important consequences for bioenergetics as approximately half of total ATP budgets is consumed directly by protein synthesis machinery [84,85]. Knowing that a typical protein has 375 amino acids [86], and that translation of a single amino acid requires roughly 6 ATPs [4] we estimate the ATP cost for *de novo* protein synthesis during hematopoiesis with the following expression:

Cost of protein synthesis for each lineage = protein synthesis requirements per lineage (proteins required per day) x number of ATPs required to translate a single protein (ATPs per protein)

$$\textbf{RBC} = (1.3 \times 10^{19}) \times\ 375\ \times\ 6 \approx 2.9\ \times 10^{22}\ ATPs\ per\ day$$

$$\textbf{M} = (3.6 \times 10^{19}) \times\ 375\ \times\ 6 \approx 8.1\ \times 10^{22}\ ATPs\ per\ day$$

Calculation 2g: How many calories are required to maintain the human RBC compartment at steady state?

At a fixed moment in time each Human RBC contains 9.7 x 10^7 ATP molecules, as determined by NMR measurements[87], with results consistent with luciferase assay measurements[88]. The major ATP consuming mechanisms in RBCs are NA/K/Ca pumps and cytoskeleton polymerization, with experimental measurements suggesting that these processes lead to an ATP turnover rate of ~1 mmol of ATP per liter of cells per hour [89–91]. The volume of an RBC is ~1 x10^{-13} Liters [92] and thus if we multiply the ATP turnover rate per liter of cells per hour with this volume, we obtain a turnover rate of 1 x10^{-16} moles of ATP per cell per hour, which can be transformed from moles into molecules:

ATP turnover rate per liter of cells (moles of ATP per liter of cells per hour) x volume of 1 cell (liters)

$$(1 \times 10^{-3})(1 \times 10^{-13}) = 1 \times 10^{-16}\ moles\ of\ ATP\ per\ cell\ per\ hour$$

Number of moles (ATP per cell per hour) x Avogadro's number =

$$(1 \times 10^{-16})(6 \times 10^{23}) = 6 \times 10^{7}\ molecules\ of\ ATP\ per\ cell\ per\ hour$$

Given there is a total of 2.5×10^{13} RBCs in humans we can multiply the ATP turnover rate by the total number of cells to estimate the energetic cost of the RBC compartment:

$$(6 \times 10^{7}) \times 24 \times (2.5 \times 10^{13}) \approx 3.6 \times 10^{22}\ molecules\ of\ ATP\ per\ day$$

To convert ATP numbers to a more familiar scale, calories, we perform the following transformation:

(Grams of glucose/molar mass of glucose) x Avogadros number = the number of glucose molecules in 1 gram of glucose

$$\frac{1}{180.2} \times (6 \times 10^{23}) = 3.3 \times 10^{21}\ molecules\ of\ glucose\ in\ 1\ gram$$

Red blood cells do not have mitochondria and must break down glucose using only glycolysis, a process which yields 2 ATPs per molecule of glucose. Therefore, in red blood cells:

$$1\ gram\ of\ glucose = (3.34\ \times 10^{21}) \times\ 2 =\ 6.7\ \times 10^{21}\ ATPs\ obtained\ by\ glycolysis$$

If the total red blood cell pool needs 3.6 x 10^{22} ATPs and 1 gram of glucose yields 6.7 x 10^{21} ATPs then the entire red blood cell compartment requires 5.4 grams of glucose ($3.6\ x\ 10^{22} \div 6.7 \times 10^{21}$). Each gram of sugar has 4kcal therefore we would need ~22 kcal to sustain RBC energetic requirements using glycolysis alone.

This value does not represent the entire caloric cost however, as it does not account for the cell divisions required to replace the number RBCs that die each day, a parameter that has yet to be measured. We estimate the caloric cost of red blood cell turnover as follows:

The total turnover rate of the red blood cell compartment has been estimated for humans, and converted into a mass scale [4]. This meta-analysis suggests that red blood cell turnover accounts for 20 grams of mass. Assuming a water content of 70% and that proteins account for 60% of dry mass we get the following estimate for the protein turnover needed for erythropoiesis:

Total mass turnover rate (grams) x % of dry mass in a cell x % of proteins in dry mass of a cell

$$20\ \times\ (1 - 0.7)\ \times 0.6 = 3.6\ grams\ of\ protein\ each\ day\ are\ needed\ to\ fuel\ RBC\ turnover$$

We can then convert this to a caloric scale using the approach described in [4]. In this scheme we assume that it takes 5kJ of energy to make 1 gram of protein[4].

Protein turnover per day x energy cost of protein synthesis

$$3.6\ \times\ 5 = 18kJ\ per\ day$$

Knowing that there are 0.24 kcal per kJ we can convert to calories:

$$18\ \times\ 0.24 = 4.3kcal$$

However, this number only considers protein synthesis, and not the entire ATP cost of making new cells. It has been estimated that protein synthesis accounts for 30% of all ATP use in cells, based on measuring the respiration rate of rat thymocytes following inhibition of different ATP-consuming processes [84]. Assuming that protein synthesis also accounts for 30% of all ATP use in erythroblasts we estimate that:

$$4.3 \times \frac{10}{3} \approx 14\ kcal\ per\ day \text{ to fuel erythropoiesis}$$

Taken together, our theoretical calculations suggest that just ~22 kcal are needed to maintain existing RBCs, while ~14kcal are needed to create new RBCs. Therefore ~36kcal, the equivalent of a single strawberry is enough to fuel erythroid homeostasis, a striking result considering 90% of the entire cellular content of the human body. However, this remains a theoretical prediction, based on a number of key assumptions (detailed above) and so warrants experimental validation.

Calculation 2h: calculating the numbers of lipids in different subsets

Leidl et al[56] have measured lipid content in different human blood cell types using ESI-MS/MS and measurements were normalized to the protein content of each cell as measured by a BCA assay[56]. In this study total lipids are based on measurements of the following: phospholipids. Phosphatidylcholine (PC), sphingomyelin (SM), phosphatidylethanolamine (PE), PE-based plasmalogens (PE-pl), phosphatidylglycerol (PG), phosphatidylinositol (PI), phosphatidylserine (PS), lysophosphatidylcholine (LPC)), ceramide (Cer), cholesteryl esters (CE) and free cholesterol (FC). As these subtypes are highly abundant [93]. In the following section we provide an example calculation showing how total lipid numbers are calculated for monocytes:

Leidl et al report there are 5.5nmol of lipids in 10^6 monocytes

Moles of lipids per cell x Avogadros number = number of lipids per monocyte

$$(5.5\ \times\ 10^{-15}) \times (6\ \times\ 10^{23}) = 3.3 \times 10^{9} lipids\ per\ monocyte$$

The same data transformation was applied to all of the other cell lineages.

Calculation 2i: calculating numbers of proteins in different subsets

Using a BCA assay Leidl *et al* [56]have quantified the amount of proteins in different hematopoietic cell types. However in this publication,the data are reported indirectly, in that they provide the amount of lipids per

mg/protein, and also the amount of lipids per 10^6 cells. Using these numbers we can identify the protein content of each cell type as follows (here we use monocytes as an example):

Leidl et al report that monocytes have 118nmol of lipids per mg/protein and there are 5.5nmol lipid per 10^6 cells.

Lipid content per mg protein ÷ amount of lipid in 10^6 cells =

0.046mg protein per 10^6 cells or 4.66×10^{-11} grams of protein per cell.

As the average protein is 52kDa (113349) or 86.32×10^{-21} grams we can infer the number of proteins by the following expression:

Total protein content ÷ size of average protein

$4.66 \times 10^{-11} \div 86.32 \times 10^{-21} = 5.4 \times 10^8$ *proteins per monocyte*

References

1 Sender, R. *et al.* (2016) Revised Estimates for the Number of Human and Bacteria Cells in the Body. *PLOS Biol.* 14, e1002533

2 Milo, R. and Phillips, R. (2015) *Cell Biology by the Numbers*, 1 edition.Garland Science.

3 Grubb, S.C. *et al.* (2009) Mouse Phenome Database. *Nucleic Acids Res.* 37, D720–D730

4 Sender, R. and Milo, R. (2021) The distribution of cellular turnover in the human body. *Nat. Med.* 27, 45–48

5 Lahoz-Beneytez, J. *et al.* (2016) Human neutrophil kinetics: modeling of stable isotope labeling data supports short blood neutrophil half-lives. *Blood* 127, 3431–3438

6 Valentin, J. (2002) Basic anatomical and physiological data for use in radiological protection: reference values: ICRP Publication 89. *Ann. ICRP* 32, 1–277

7 Makarieva, A.M. *et al.* (2008) Mean mass-specific metabolic rates are strikingly similar across life's major domains: Evidence for life's metabolic optimum. *Proc. Natl. Acad. Sci. U. S. A.* 105, 16994–16999

8 Trepel, F. (1974) Number and distribution of lymphocytes in man. A critical analysis. *Klin. Wochenschr.* 52, 511–515

9 Qatarneh, S.M. *et al.* (2006) Three-dimensional atlas of lymph node topography based on the visible human data set. *Anat. Rec. B. New Anat.* 289, 98–111

10 Busch, K. *et al.* (2015) Fundamental properties of unperturbed haematopoiesis from stem cells in vivo. *Nature* 518, 542–546

11 Wilson, N.K. *et al.* (2015) Combined Single-Cell Functional and Gene Expression Analysis Resolves Heterogeneity within Stem Cell Populations. *Cell Stem Cell* 16, 712–724

12 Challen, G.A. *et al.* (2010) Distinct Hematopoietic Stem Cell Subtypes Are Differentially Regulated by TGFβ1. *Cell Stem Cell* 6, 265–278

13 Beerman, I. *et al.* (2010) Functionally distinct hematopoietic stem cells modulate hematopoietic lineage potential during aging by a mechanism of clonal expansion. *Proc. Natl. Acad. Sci. U. S. A.* 107, 5465–5470

14 Sawai, C.M. *et al.* (2016) Hematopoietic Stem Cells Are the Major Source of Multilineage Hematopoiesis in Adult Animals. *Immunity* 45, 597–609

15 Pei, W. *et al.* (2020) Resolving Fates and Single-Cell Transcriptomes of Hematopoietic Stem Cell Clones by PolyloxExpress Barcoding. *Cell Stem Cell* 27, 383-395.e8

16 Rodriguez-Fraticelli, A.E. *et al.* (2020) Single-cell lineage tracing unveils a role for TCF15 in haematopoiesis. *Nature* 583, 585–589

17 Bowling, S. *et al.* (2020) An Engineered CRISPR-Cas9 Mouse Line for Simultaneous Readout of Lineage Histories and Gene Expression Profiles in Single Cells. *Cell* 181, 1410-1422.e27

18 Sun, J. *et al.* (2014) Clonal dynamics of native haematopoiesis. *Nature* 514, 322–327

19 Abkowitz, J.L. *et al.* (2002) Evidence that the number of hematopoietic stem cells per animal is conserved in mammals. *Blood* 100, 2665–2667

20 Lee-Six, H. *et al.* (2018) Population dynamics of normal human blood inferred from somatic mutations. *Nature* 561, 473–478

21 Watson, C.J. *et al.* (2020) The evolutionary dynamics and fitness landscape of clonal hematopoiesis. *Science* 367, 1449–1454

22 Biasco, L. *et al.* (2016) In Vivo Tracking of Human Hematopoiesis Reveals Patterns of Clonal Dynamics during Early and Steady-State Reconstitution Phases. *Cell Stem Cell* 19, 107–119

23 Sommerkamp, P. *et al.* (2021) Mouse multipotent progenitor 5 cells are located at the interphase between hematopoietic stem and progenitor cells. *Blood* 137, 3218–3224

24 Morrison, S.J. and Weissman, I.L. (1994) The long-term repopulating subset of hematopoietic stem cells is deterministic and isolatable by phenotype. *Immunity* 1, 661–673

25 Morrison, S.J. *et al.* (1997) Identification of a lineage of multipotent hematopoietic progenitors. *Dev. Camb. Engl.* 124, 1929–1939

26 Akashi, K. *et al.* (2000) A clonogenic common myeloid progenitor that gives rise to all myeloid lineages. *Nature* 404, 193–197

27 Nakorn, T.N. *et al.* (2003) Characterization of mouse clonogenic megakaryocyte progenitors. *Proc. Natl. Acad. Sci.* 100, 205–210

28 Harman, B.C. *et al.* (2008) Resolution of Unique Sca-1 ^{high} c-Kit $^{-}$ Lymphoid-Biased Progenitors in Adult Bone Marrow. *J. Immunol.* 181, 7514–7524

29 Kumar, R. *et al.* (2008) Lin−Sca1+Kit− Bone Marrow Cells Contain Early Lymphoid-Committed Precursors That Are Distinct from Common Lymphoid Progenitors. *J. Immunol.* 181, 7507–7513

30 Giandomenico, S.D. *et al.* (2019) Megakaryocyte TGFβ1 Partitions Hematopoiesis into Immature Progenitor/Stem Cells and Maturing Precursors. *bioRxiv* DOI: 10.1101/689901

31 Kirby, M.R. and Donahue, R.E. (1993) Rare Event Sorting of CD34+ Hematopoietic Cells. *Ann. N. Y. Acad. Sci.* 677, 413–416

32 Hao, Q.-L. *et al.* (1995) A Functional Comparison of CD34+ CD38– Cells in Cord Blood and Bone Marrow. *Blood* 86, 3745–3753

33 Farrell, T. *et al.* (2014) Changes in the frequencies of human hematopoietic stem and progenitor cells with age and site. *Exp. Hematol.* 42, 146–154

34 Povsic, T.J. *et al.* (2010) Aging is not associated with bone marrow-resident progenitor cell depletion. *J. Gerontol. A. Biol. Sci. Med. Sci.* 65, 1042–1050

35 Boyer, S.W. *et al.* (2019) Clonal and Quantitative In Vivo Assessment of Hematopoietic Stem Cell Differentiation Reveals Strong Erythroid Potential of Multipotent Cells. *Stem Cell Rep.* 12, 801–815

36 Niswander, L.M. *et al.* (2014) Improved quantitative analysis of primary bone marrow megakaryocytes utilizing imaging flow cytometry. *Cytometry A* 85, 302–312

37 Basilico, S. and Göttgens, B. (2017) Dysregulation of haematopoietic stem cell regulatory programs in acute myeloid leukaemia. *J. Mol. Med. Berl. Ger.* 95, 719–727

38 Krueger, A. *et al.* (2017) T Cell Development by the Numbers. *Trends Immunol.* 38, 128–139

39 Romar, G.A. *et al.* (2016) Research Techniques Made Simple: Techniques to Assess Cell Proliferation. *J. Invest. Dermatol.* 136, e1–e7

40 Wilson, A. *et al.* (2008) Hematopoietic stem cells reversibly switch from dormancy to self-renewal during homeostasis and repair. *Cell* 135, 1118–1129

41 Akinduro, O. *et al.* (2018) Proliferation dynamics of acute myeloid leukaemia and haematopoietic progenitors competing for bone marrow space. *Nat. Commun.* 9, 519

42 Takahashi, M. *et al.* (2021) Reconciling Flux Experiments for Quantitative Modeling of Normal and Malignant Hematopoietic Stem/Progenitor Dynamics. *Stem Cell Rep.* 16, 741–753

43 Signer, R.A.J. *et al.* (2016) The rate of protein synthesis in hematopoietic stem cells is limited partly by 4E-BPs. *Genes Dev.* 30, 1698–1703

44 Catlin, S.N. *et al.* (2011) The replication rate of human hematopoietic stem cells in vivo. *Blood* 117, 4460–4466

45 Borghans, J.A.M. *et al.* (2018) Current best estimates for the average lifespans of mouse and human leukocytes: reviewing two decades of deuterium-labeling experiments. *Immunol. Rev.* 285, 233–248

46 Ballesteros, I. *et al.* (2020) Co-option of Neutrophil Fates by Tissue Environments. *Cell* 183, 1282-1297.e18

47 Verheijen, M. *et al.* (2020) Fate Mapping Quantifies the Dynamics of B Cell Development and Activation throughout Life. *Cell Rep.* 33,

48 Bernitz, J.M. *et al.* (2016) Hematopoietic Stem Cells Count and Remember Self-Renewal Divisions. *Cell* 167, 1296-1309.e10

49 Chambers, S.M. *et al.* (2007) Aging hematopoietic stem cells decline in function and exhibit epigenetic dysregulation. *PLoS Biol.* 5, e201

50 Harker, L.A. and Finch, C.A. (1969) Thrombokinetics in man. *J. Clin. Invest.* 48, 963–974

51 Amann-Zalcenstein, D. *et al.* (2020) A new lymphoid-primed progenitor marked by Dach1 downregulation identified with single cell multi-omics. *Nat. Immunol.* 21, 1574–1584

52 Model, M.A. (2018) Methods for cell volume measurement. *Cytometry A* 93, 281–296

53 Hidalgo San Jose, L. *et al.* (2020) Modest Declines in Proteome Quality Impair Hematopoietic Stem Cell Self-Renewal. *Cell Rep.* 30, 69-80.e6

54 Signer, R.A.J. *et al.* (2014) Haematopoietic stem cells require a highly regulated protein synthesis rate. *Nature* 509, 49–54

55 Agathocleous, M. *et al.* (2017) Ascorbate regulates haematopoietic stem cell function and leukaemogenesis. *Nature* 549, 476–481

56 Leidl, K. *et al.* (2008) Mass spectrometric analysis of lipid species of human circulating blood cells. *Biochim. Biophys. Acta BBA - Mol. Cell Biol. Lipids* 1781, 655–664

57 Radley, J.M. *et al.* (1999) Ultrastructure of primitive hematopoietic stem cells isolated using probes of functional status. *Exp. Hematol.* 27, 365–369

58 Noris, P. *et al.* (2014) Platelet diameters in inherited thrombocytopenias: analysis of 376 patients with all known disorders. *Blood* 124, e4–e10

59 H, D. *et al.* (2011) Normal range of mean platelet volume in healthy subjects: Insight from a large epidemiologic study. *Thromb. Res.* 128,

60 Bessman, J.D. (1984) The relation of megakaryocyte ploidy to platelet volume. *Am. J. Hematol.* 16, 161–170

61 Mclaren, C.E. *et al.* (1987) Statistical and graphical evaluation of erythrocyte volume distributions. *Am. J. Physiol. 252 Heart Circ. Physiol.*

62 Downey, G.P. *et al.* (1990) Retention of leukocytes in capillaries: role of cell size and deformability. *J. Appl. Physiol. Bethesda Md 1985* 69, 1767–1778

63 Ting-Beall, H.P. *et al.* (1993) Volume and osmotic properties of human neutrophils. *Blood* 81, 2774–2780

64 Needham, D. and Hochmuth, R.M. (1990) Rapid flow of passive neutrophils into a 4 microns pipet and measurement of cytoplasmic viscosity. *J. Biomech. Eng.* 112, 269–276

65 Kuse, R. *et al.* (1985) Blood lymphocyte volumes and diameters in patients with chronic lymphocytic leukemia and normal controls. *Blut* 50, 243–248

66 Chervenick, P.A. *et al.* (1968) Quantitative studies of blood and bone marrow neutrophils in normal mice. *Am. J. Physiol.* 215, 353–360

67 Méndez-Ferrer, S. *et al.* (2010) Mesenchymal and haematopoietic stem cells form a unique bone marrow niche. *Nature* 466, 829–834

68 Worthley, D.L. *et al.* (2015) Gremlin 1 Identifies a Skeletal Stem Cell with Bone, Cartilage, and Reticular Stromal Potential. *Cell* 160, 269–284

69 Zhou, B.O. *et al.* (2014) Leptin-Receptor-Expressing Mesenchymal Stromal Cells Represent the Main Source of Bone Formed by Adult Bone Marrow. *Cell Stem Cell* 15, 154–168

70 Gomariz, A. *et al.* (2018) Quantitative spatial analysis of haematopoiesis-regulating stromal cells in the bone marrow microenvironment by 3D microscopy. *Nat. Commun.* 9, 2532

71 Menees, K.B. *et al.* (2021) Sex- and age-dependent alterations of splenic immune cell profile and NK cell phenotypes and function in C57BL/6J mice. *Immun. Ageing* 18, 3

72 Kaliss, N. and Pressman, D. (2016) Plasma and Blood Volumes of Mouse Organs, As Determined with Radioactive Iodoproteins.∗: *Proc. Soc. Exp. Biol. Med.* DOI: 10.3181/00379727-75-18083

73 Furth, J. and Sobel, H. (1946) Hypervolemia Secondary to Grafted Granulosa-Cell Tumor2. *JNCI J. Natl. Cancer Inst.* 7, 103–113

74 Keighley, G. *et al.* (1962) Response of Normal and Genetically Anaemic Mice to Erythropoietic Stimuli*. *Br. J. Haematol.* 8, 429–441

75 Riches, A.C. *et al.* (1973) Blood volume determination in the mouse. *J. Physiol.* 228, 279–284

76 Sluiter, W. *et al.* (1984) Determination of blood volume in the mouse with 51Chromium-labelled erythrocytes. *J. Immunol. Methods* 73, 221–225

77 Van den Broeck, W. *et al.* (2006) Anatomy and nomenclature of murine lymph nodes: Descriptive study and nomenclatory standardization in BALB/cAnNCrl mice. *J. Immunol. Methods* 312, 12–19

78 Kawashima, Y. *et al.* (1964) The lymph system in mice. *Subj. Strain Bibliogr. 1964*

79 Druzd, D. *et al.* (2017) Lymphocyte Circadian Clocks Control Lymph Node Trafficking and Adaptive Immune Responses. *Immunity* 46, 120–132

80 Hsu, H.-C. *et al.* (2003) Age-related thymic involution in C57BL/6J × DBA/2J recombinant-inbred mice maps to mouse chromosomes 9 and 10. *Genes Immun.* 4, 402–410

81 Allman, D.M. *et al.* (1993) Peripheral B cell maturation. II. Heat-stable antigen(hi) splenic B cells are an immature developmental intermediate in the production of long-lived marrow-derived B cells. *J. Immunol. Baltim. Md 1950* 151, 4431–4444

82 Kaufman, R.M. *et al.* (1965) Circulating megakaryocytes and platelet release in the lung. *Blood* 26, 720–731

83 Trowbridge, E.A. *et al.* (1984) The origin of platelet count and volume. *Clin. Phys. Physiol. Meas. Off. J. Hosp. Phys. Assoc. Dtsch. Ges. Med. Phys. Eur. Fed. Organ. Med. Phys.* 5, 145–170

84 Buttgereit, F. and Brand, M.D. (1995) A hierarchy of ATP-consuming processes in mammalian cells. *Biochem. J.* 312, 163–167

85 Argüello, R.J. *et al.* (2020) SCENITH: A Flow Cytometry-Based Method to Functionally Profile Energy Metabolism with Single-Cell Resolution. *Cell Metab.* 32, 1063-1075.e7

86 Brocchieri, L. and Karlin, S. (2005) Protein length in eukaryotic and prokaryotic proteomes. *Nucleic Acids Res.* 33, 3390–3400

87 Sarpel, G. *et al.* (1982) Erythrocyte phosphate content in Huntington's disease. *Neurosci. Lett.* 31, 91–96

88 Thore, A. *et al.* (1975) Detection of bacteriuria by luciferase assay of adenosine triphosphate. *J. Clin. Microbiol.* 1, 1–8

89 Lew, V.L. and Tiffert, T. (2017) On the Mechanism of Human Red Blood Cell Longevity: Roles of Calcium, the Sodium Pump, PIEZO1, and Gardos Channels. *Front. Physiol.* 8, 977
90 Müller, E. *et al.* (1986) Turnover of phosphomonoester groups and compartmentation of polyphosphoinositides in human erythrocytes. *Biochem. J.* 235, 775–783
91 Feig, S.A. *et al.* (1972) Energy metabolism in human erythrocytes. *J. Clin. Invest.* 51, 1547–1554
92 Child, J.A. *et al.* (1967) A diffraction method for measuring the average volumes and shapes of red blood cells. *Br. J. Haematol.* 13, 364–375
93 van Meer, G. *et al.* (2008) Membrane lipids: where they are and how they behave. *Nat. Rev. Mol. Cell Biol.* 9, 112–124
94 Bogue, M.A. *et al.* (2020) Mouse Phenome Database: a data repository and analysis suite for curated primary mouse phenotype data. *Nucleic Acids Res.* 48, D716–D723
95 Kawashima, Y. *et al.* (1964) THE LYMPH SYSTEM IN MICE.
96 Druzd, D. *et al.* (2017) Lymphocyte Circadian Clocks Control Lymph Node Trafficking and Adaptive Immune Responses. *Immunity* 0,
97 Tanaka, S. *et al.* (2020) Tet2 and Tet3 in B cells are required to repress CD86 and prevent autoimmunity. *Nat. Immunol.* 21, 950–961